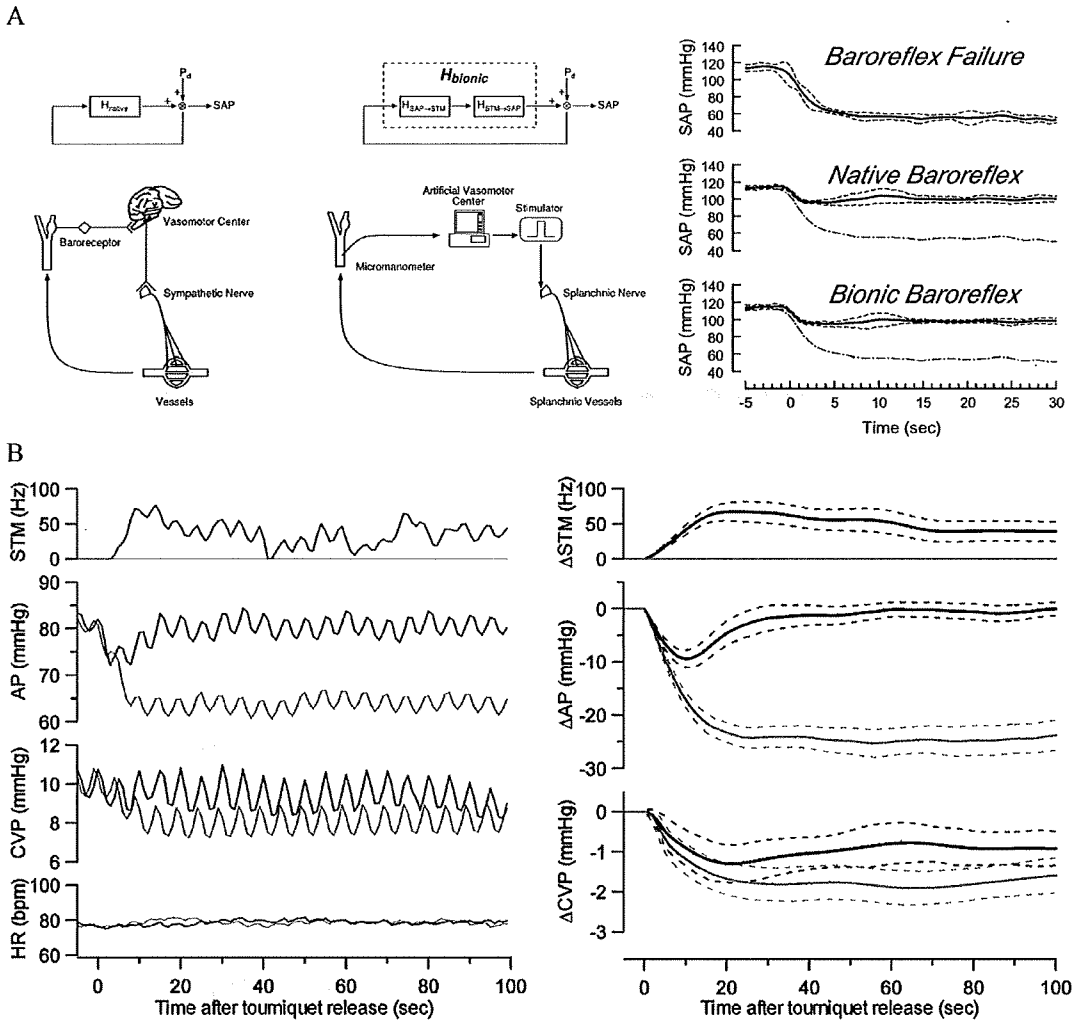

Fig. 6. (A) Functional and anatomical diagram of native baroreflex (left) and bionic baroreflex (center). Pd: pressure perturbation; SAP: systemic arterial pressure; H_{native}: open-loop transfer function of native baroreflex; H_{bionic}: open-loop transfer function of total bionic baroreflex; $H_{SAP \rightarrow STM}$: transfer function of designed bionic baroreflex controller; $H_{STM \rightarrow SAP}$: transfer function of native baroreflex plant. Changes in SAP in baroreflex failure, native baroreflex, and bionic baroreflex after head-up tilt (right). Dash-dot lines: average response in baroreflex failure. (B) Hypotension after tourniquet release was prevented by bionic baroreflex system using epidural spinal cord stimulation. Left: a representative patient; right: pooled data from 21 patients. STM: stimulation frequency; AP: arterial pressure; CVP: central venous pressure, HR: heart rate. (Reproduced from [5], [6] (A) and [72] (B) with permission.)

Yanagiya *et al.* [71] constructed a bionic baroreflex system using spinal cord stimulation via an epidural electrode catheter in six cats. They [71] designed the controller to provide quick and stable control only, rather than to mimic the biological controller. The system ameliorated a drop in pressure from 37 ± 5 to 21 ± 2 mmHg at 5 s and 59 ± 11 to 8 ± 4 mmHg at 30 s ($p < 0.05$). Epidural spinal-cord stimulation was further clinically applied by Yamasaki *et al.* [72] during surgery in a selected group of patients ($n = 12$) undergoing knee surgery. Pressure drop after tourniquet deflation was suppressed significantly ($p < 0.05$) from 17 ± 3 to 9 ± 2 mmHg at 10 s and 25 ± 2 to 1 ± 2 mmHg at 50 s [Fig. 6(B)]. Various inputs other than direct sympathetic stimulation may change blood pressure [67]–[70], [73]–[75]. Even noninvasive transcutaneous electrical stimulation [76] was developed for suppressing hypotension in patients with spinal-cord injury. In 12 patients, bionic feedback control restored the pressure drop by 50% in 35 ± 12 s and by 90% in 60 ± 18 s.

VI. Treatment of Heart Failure

A. Neurohormonal Activation Plays Major Roles in the Pathogenesis of Heart Failure

Heart failure is a complex syndrome that can result from any kind of cardiac diseases at their advanced stage. Mortality with this syndrome is considerably high even with the development of state-of-art treatments including artificial hearts, regenerative medicine, and cardiac transplantation. Recently, implantable device-based treatment of heart failure has attracted physicians' interest because of its enormous impact on survival. Available devices include implantable cardiac defibrillator to terminate fatal arrhythmia and cardiac resynchronization treatment device to improve the synchronicity of left ventricular contraction and hence cardiac performance. Device for bionic treatment of heart failure is now under aggressive development to complement the roles of these devices.

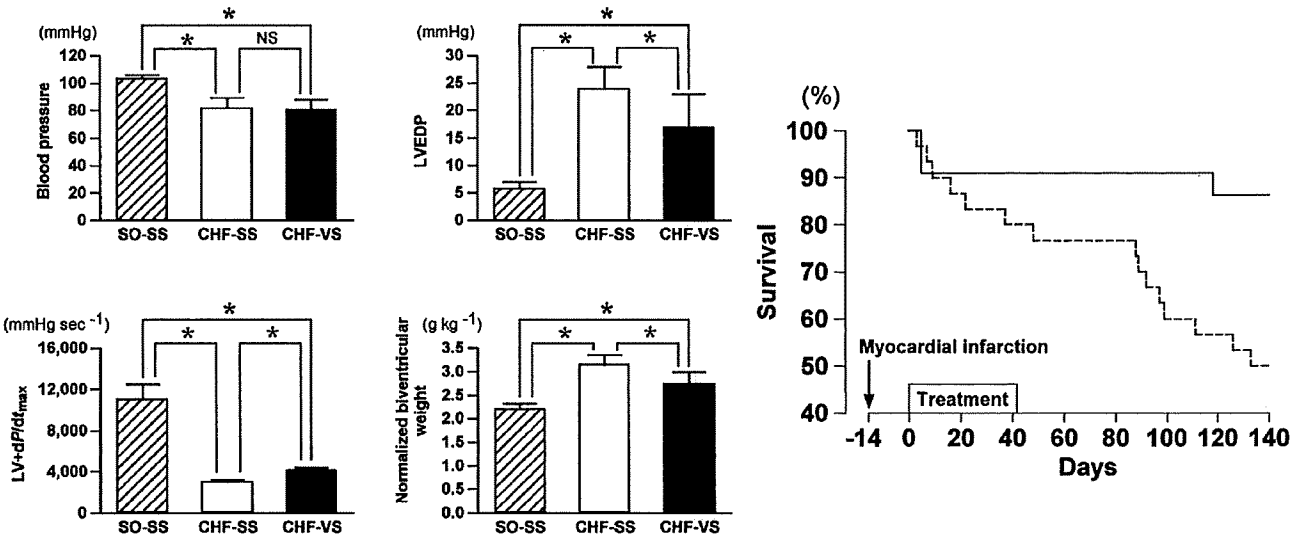

Fig. 7. Forty-two-day right vagal stimulation attenuated increased LVEDP, decreased maximal rate of left ventricular pressure rise (LV $+dP/dt_{max}$), increased normalized biventricular weight (left). SO-SS: sham-stimulated rats without failure (n = 9); CHF-SS: sham-stimulated rats with heart failure (n = 13); CHF-VS: vagal-stimulated rats with heart failure (n = 11); (*) $p < 0.05$. Survival for 140 days of rats with (solid line, n = 22) or without (dashed line, n = 30) 42-day vagal stimulation (right). (Reproduced from [78] with permission.)

Although the primary cause of heart failure is decreased pump function, the adjunct neurohumoral activation is certainly a major aggravating factor for disease progression and risk of death. Clinical trials on drugs for heart failure have revealed repeatedly that suppression of neurohumoral factors rather than increasing cardiac contractility improves survival. Pharmacological activation of vagal tone (such as low-dose scopolamine) [77] has been evaluated, but the effects on long-term survival have not been shown. With this background, bionic device therapy counteracting activated neurohumoral factors has been developed.

B. *Vagal Nerve Stimulation in Animal Studies*

Li *et al.* [78] first demonstrated that direct electrical stimulation of right vagal nerve (started after healing of extensive myocardial infarction) was effective in delaying the progression of heart failure and drastically improving survival in rats with heart failure. The intensity of vagal stimulation was low (decreasing heart rate by approximately 10%) enough to avoid adverse effects. They showed that vagal stimulation (control, n = 13; vagal stimulation, n = 11) significantly decreased left ventricular filling pressure from 24 ± 4 to 17 ± 6 mmHg, increased left ventricular $+dp/dt_{max}$ from 2987 $\pm$ 192 to 4152 ± 37 mmHg/s and decreased biventricular weight from 3.1 ± 0.2 to 2.8 ± 0.3 g/kg body weight, although the size of infarction was unchanged. Vagal nerve stimulation markedly improved survival from 50% to 82% ($p < 0.01$) at 140 days (Fig. 7). The same group also showed that vagal stimulation suppressed arrhythmias [79] and decreased both vasopressin secretion and salt ingestion [80]. The latter indicates the possible contribution of central modification induced by afferent nerve stimulation. Heart rate decreased progressively in six weeks. Vagal nerve stimulation protected the heart against acute ischemia, as well as reduced norepinephrine [81] and myoglobin [82] (an index of myocardial injury) release. These effects were attributed to its bradycardiac effect. Uemura *et al.* [83] investigated the effect of vagal nerve stimulation (−15 to 240 min) on matrix metalloproteinase (MMP) activity in a rabbit model of ischemia (60 min)-reperfusion (180 min) injury. Vagal stimulation increased the expression of tissue inhibitor of MMP-1 (TIMP-1) in cardiomyocytes and reduced active MMP-9. These molecular mechanisms of vagal stimulation might help prevent cardiac remodeling.

Some of the beneficial effects of vagal stimulation in heart failure may involve anti-inflammatory pathways. A large body of evidence [84]–[89] indicates that both afferent and efferent vagal nerves form anti-inflammatory pathways. The afferent vagal nerve senses local inflammation and transmits the information to the brain to suppress excessive inflammatory response in other areas in which inflammation may be elicited by the diffusion of various cytokines. In addition to recruiting the hypothalamic-pituitary-adrenal axis to release corticoids, the efferent vagal nerve is activated for faster anti-inflammatory response. The efferent activity stimulates nicotinic receptors on macrophages [84], and nicotinic alpha7 unit is essential for this regulation [86]. Activation of nicotinic receptors inhibits the release of pro-inflammatory cytokines such as TNF-alpha, IL-5, and IL-18 but does not inhibit the anti-inflammatory cytokine IL-10 [84]. Efferent vagal nerve stimulation is shown to decrease liver NF-kappa B, reduce plasma TNF-alpha, and revert hypotension in hemorrhagic shock (besides septic shock) through nicotinic receptors [89]. These findings indicate the involvement of inflammatory response in life-threatening cardiovascular disease such as hemorrhagic shock and heart failure.

C. *Vagal Nerve Stimulation in Patients With Heart Failure*

Recently, an implantable chronic vagal neurostimulator has entered clinical trial [90]. In this small-sized trial, the stimu-

lator (Cardiofit, BioControl) was implanted in 32 patients with heart failure (NYHA II to III, ejection fraction $\leq$ 35%). The right vagal nerve was stimulated intermittently (4 mA, 21% on). Heart rate decreased from 82 to 76 bpm; quality-of-life score (Minnesota Living with Heart Failure Questionnaire) improved from 48 to 32; 6-min walk increased from 410 to 471 m; and left ventricular ejection fraction increased from 23% to 27% in six months. The impact of vagal stimulation on the hard endpoint in these patients remains to be seen.

D. Carotid Sinus Nerve Stimulation in Heart Failure

Zucker *et al.* [91] examined if carotid sinus nerve stimulation (CVRx) improves the survival of dogs with pacing-induced (250 bpm) heart failure. They continued tachypacing until the endpoint (death or moribund state) was reached. Although the progression of heart failure (indicated by left ventricular end-diastolic pressure, left ventricular $+dp/dt_{max}$, mean arterial pressure, heart rate, ejection fraction) was similar between dogs with and without carotid sinus nerve stimulation, increases in norepinephrine and angiotensin II were delayed in dogs with carotid sinus nerve stimulation. Dogs with carotid sinus nerve stimulation survived longer. How this observation translates to the clinical impact of carotid sinus nerve stimulation in patients with heart failure remains to be investigated.

VII. Autopilot Treatment of Acute Decompensated Heart Failure

Although neurohumoral suppression is the mainstay of long-term treatment for heart failure, a different strategy is required when the hemodynamics are acutely exacerbated. In order to save the lives of such patients, vital hemodynamic variables including blood pressure, cardiac output, and left atrial pressure have to be maintained within physiological ranges. Abnormality in each of these variables should be corrected promptly. The management of hemodynamic decompensation requires complex control of infusions of multiple potent drugs. The advent of automated feedback control of multiple drug infusions would have a major impact on clinical medicine. Such closed-loop feedback treatment involves control engineering and electronic controllers. This is also an important area of bionic cardiology.

A. Development of Integrative Cardiovascular Model

Various modalities of feedback control of hemodynamic variables using drug infusion have been attempted [92], [93], including those that control two variables. These attempts were only partially successful due to the complex interaction between variables. Results of these investigations prompted Uemura *et al.* [94], [97], [98] to take a different approach for hemodynamic control. They first established methods to break down each hemodynamic variable into fundamental physiological properties of the cardiovascular system. This was achieved by modeling the total cardiovascular system as the interaction of three different components: left heart pump, right heart pump, and total (systemic and pulmonary) vasculature [94], [96]. The model is an extension of Guyton's cardiovascular model [95] but differs from Guyton's model in several aspects: a third axis is incorporated to explicitly express left atrial pressure; the left and right heart pump functions are defined independently; and blood redistribution between systemic and pulmonary vasculature is expressed on the same venous return surface [Fig. 8(A)]. Using this model, Uemura *et al.* [94], [97] succeeded in delineating fundamental determinants of hemodynamics (left heart pump function, right heart pump function, systemic vascular resistance, and total stressed blood volume) from clinically measurable variables (blood pressure, cardiac output, left atrial pressure, and right atrial pressure).

B. Bionic Treatment of Decompensated Heart Failure

Based on their new model, Uemura *et al.* [98] designed a bionic controller that can simultaneously normalize blood pressure, cardiac output, and left atrial pressure accurately, quickly, and stably [Fig. 8(B)]. Their success is based on the effective decoupling of the complex interaction between variables, thereby allowing them to design three independent feedback control loops: left heart pump function controlled by an inotropic agent (dobutamine), systemic vascular resistance controlled by a vasodilator (sodium nitroprusside), and total stressed blood volume controlled by a volume expander and/or a diuretic (dextran solution, furosemide). Using the controller in 12 anesthetized dogs with severely decompensated heart failure restored the pump function, vascular resistance, and blood volume to normal levels in 30 min. As a result, blood pressure was controlled within 4.4 ± 2.6 mmHg, cardiac output within 5.4 ± 2.4 ml/min/Kg, and left atrial pressure within 0.8 ± 0.6 mmHg for another 30 min. The average amounts of drug use was dobutamine 4.7 ± 2.6 μg/min/kg, nitroprusside 4.2 ± 1.8 μg/min/kg, dextran infusion 2.4 ± 1.9 mL/kg, and furosemide 10 mg in one dog and 20 mg in another dog [Fig. 8(C)]. Even using the classical proportional-integral control for dobutamine and nitroprusside infusions and the "if-then" rule control for dextran/furosemide, control of multiple hemodynamic variables was possible and of good quality.

C. Beyond Hemodynamic Stabilization

Uemura *et al.* [99] attempted to further elaborate the treatment of decompensated heart failure beyond hemodynamic stabilization. They added myocardial oxygen consumption as an additional target for electronic control. The heart is an organ that consumes a large amount of oxygen and is highly vulnerable to oxygen shortage. Hayashida *et al.* [100] have shown in conscious dogs that the heart optimizes its metabolic efficiency during exercise as well as at rest. Theoretically, the optimal heart rate minimizes oxygen consumption for a given blood pressure, cardiac output, and left atrial pressure [101]. Uemura *et al.* [99] demonstrated in conscious dogs with acute decompensated heart failure that the automated electronic system of hemodynamic management allowed them to pharmacologically lower heart rate and myocardial oxygen consumption without compromising hemodynamics. The model-based approach to simultaneous optimization of multiple variables would help improve the outcome of patients with hemodynamic decompensation.

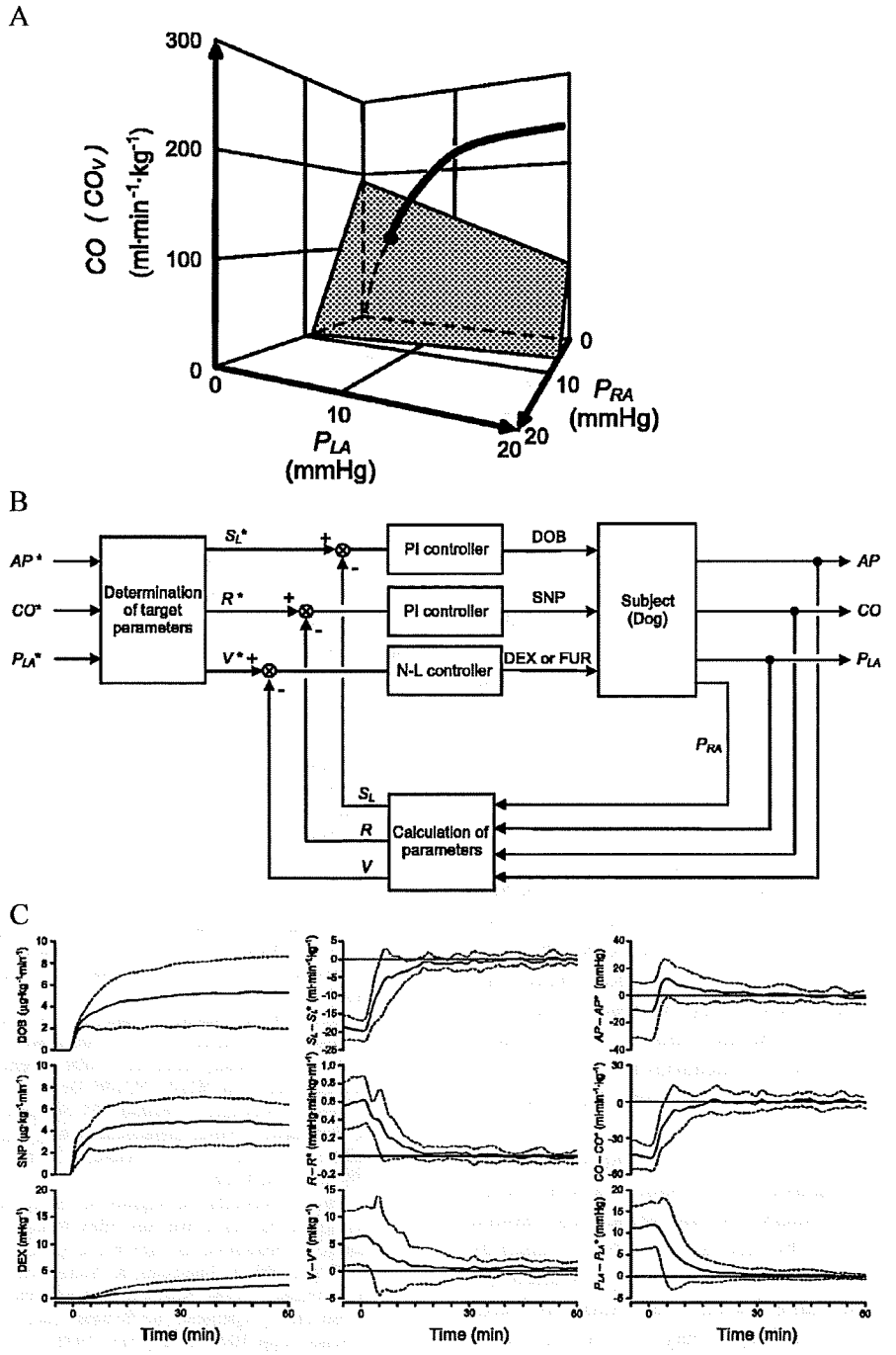

Fig. 8. (A) Extended Guyton's model of the total cardiovascular system. A third axis explicitly expresses left atrial pressure (P_{LA}), a cardiac output curve expresses left and right heart pump function independently, and a venous return surface expresses blood distribution in vasculatures. P_{RA}: right atrial pressure; CO: cardiac output; CO_V: venous return (= cardiac output). (B) Block diagram of an autopilot system for simultaneous control of systemic arterial pressure (AP), CO, and P_{LA}. Parameters with (*) indicate target values. From target variables, target values of left heart pump function (S_L), stressed blood volume (V), and systemic vascular resistance (R) are determined. S_L, V, and R of subjects are calculated from measured AP, CO, P_{LA}, and P_{RA}. Proportional-integral (PI) controllers adjust infusion rate of dobutamine (DOB) and sodium nitroprusside (SNP) to minimize the error in S_L and R, respectively. If-then rules adjust infusion of 10% dextran 40 (DEX) or injection of furosemide (FUR) to minimize the error in V. (C) Automatic correction of acute decompensated heart failure. Errors in cardiovascular properties (middle panels) (S_L, R, V) rapidly approached to zero, resulting in cardiovascular variables (right panels) (AP, CO, P_{LA}) approaching respective target. Left panels indicate infusion rate of DOB, SNP, and infused volume of DEX. (Reproduced from [98] with permission.)

VIII. Future of Bionic Medicine

We foresee a promising future for bionic medicine. It appears, however, that various factors may significantly influence the development and promotion of bionic cardiology. The first is the technology to interface native regulatory systems with bionic systems. The latest technology has made it possible to physically interface electronic devices with cardiac tissues (pacemaker, ICD). Neural interface, however, leaves much room for

improvement in terms of selectivity, stability, and durability. Sophistication of physical as well as logical neural interface will no doubt facilitate intricate body control. An advanced interface that allows stimulation at lower electrical power by minimizing current leakage and fully utilizing native excitation function will reduce adverse effects. Appropriate methods for the selective measurement and/or stimulation of subgroup of nerve fibers are necessary to match the spatial resolution indicated by the physiological/medical requirements. Autonomic function may be the first controllable function in the clinical setting compared to sensory or motor functions where intricate neural interface for higher spatial and temporal resolution is mandatory.

The second is the development of implantable long-term sensors. This factor would appear to be one of the basic needs, but has been relatively ignored until recently. For years, measurements have been limited to electrical signals. No durable sensors for mechanical or chemical variables are available. Once implanted, it is necessary to keep its accuracy even in blood for a considerably long term without repeated recalibrations. Therefore, the requirements of such sensors include long-term durability, stability, anticoagulation nature, and no need for recalibration.

The third is technology to support communication mechanisms in the body. Since the operation of bionic system is based on a closed feedback mechanism, various feedback loop components including sensors, controllers, actuators and plant have to communicate mutually. In the body, the neurohormonal mechanisms support this communication. In the bionic system, however, if some of these components are physically distant from each other, artificial communication mechanisms are needed for closed loop operation. We await the development of such an artificial communication mechanism in the body. The communication should simultaneous satisfy the short delay time (for real-time operation and closed-loop feedback), the sufficient bandwidth (depending on the application), the avoidance from interference from other communications and noises (guaranteeing secure feedback operation), and the mission-critical security (for medical need).

The fourth is the mechanism to support the power of bionic devices. This has been a significant problem, and will remain a target for research. The battery life should be long enough to be clinically meaningful. The size is preferable as small as possible. This is because the size of power supplies often determines that of the implantable devices. The third and fourth technology, if realized and combined, may obviate the use of leads, the most fragile part of implantable devices.

The fifth is the development of integrative science for biological system. To design elaborate feedback regulation of the cardiovascular system, in-depth knowledge of biological regulation is essential. Moreover, as already discussed in the Introduction, we have to go beyond the restoration of biological regulation to combat common diseases. Biological regulation has to be translated into and expressed in the "language" of control engineering. The expression should include dynamic, multiple-input, interactive, nonlinear, and feedback natures of the total system concerned. Besides these, we have to develop a model incorporating the effect of modifying biological regulation on the progression of common diseases. The development of such a model definitely requires biological research. Investigations of integrative biological regulation mandate the knowledge of both biology and engineering. It is our hope that many biomedical engineers will participate in the exploration into the development of bionic medicine.

The last factor is medical needs. Recent interest in device-based therapy will uncover the potential of bionic medicine in meeting the unmet needs. Of various cardiovascular diseases presented in this paper, the need for the appropriate treatment of chronic heart failure is most seriously unmet. Device-based therapy including bionic medicine is expected to complement existing treatment modalities to provide therapeutic benefits that cannot be achieved by drugs alone, especially for the increasing patients of chronic heart failure.

In conclusion, bionic medicine is the science to explore the wealth of controllable body parts. Bionic cardiology has a long history, through which we have accumulated much experience, generated knowledge on biological regulation, and identified unmet needs. These unique features together put us in a strong position to promote the development of more sophisticated device-based therapy for otherwise untreatable diseases. Bionic medicine will inspire more intricate applications in the twenty-first century.

REFERENCES

[1] T. Kawada and M. Sugimachi, "Artificial neural interfaces for bionic cardiovascular treatments," *J. Artif. Organs*, vol. 12, no. 1, pp. 17–22, Mar. 2009.

[2] M. Sugimachi and K. Sunagawa, "Bionic cardiovascular medicine. Functional replacement of native cardiovascular regulation and the correction of its abnormality," *IEEE Eng. Med. Biol. Mag.*, vol. 24, pp. 24–31, Jul.-Aug. 2005.

[3] T. Kubota, H. Chishaki, T. Yoshida, K. Sunagawa, A. Takeshita, and Y. Nose, "How to encode arterial pressure into carotid sinus nerve to invoke natural baroreflex," *Amer. J. Physiol.*, vol. 263, no. 1, pp. H307–H313, Jul. 1992.

[4] Y. Ikeda, M. Sugimachi, T. Yamasaki, O. Kawaguchi, T. Shishido, T. Kawada, J. Alexander Jr., and K. Sunagawa, "Explorations into development of a neurally regulated cardiac pacemaker," *Amer. J. Physiol.*, vol. 269, no. 6, pp. H2141–H2146, Dec. 1995.

[5] T. Sato, T. Kawada, T. Shishido, M. Sugimachi, J. Alexander Jr., and K. Sunagawa, "Novel therapeutic strategy against central baroreflex failure: A bionic baroreflex system," *Circulation*, vol. 100, no. 3, pp. 299–304, Jul. 1999.

[6] T. Sato, T. Kawada, M. Sugimachi, and K. Sunagawa, "Bionic technology revitalizes native baroreflex function in rats with baroreflex failure," *Circulation*, vol. 106, no. 6, pp. 730–734, Aug. 2002.

[7] M. Sugimachi, T. Imaizumi, K. Sunagawa, Y. Hirooka, K. Todaka, A. Takeshita, and M. Nakamura, "A new method to identify dynamic transduction properties of aortic baroreceptors," *Amer. J. Physiol.*, vol. 258, no. 3, pp. H887–H895, Mar. 1990.

[8] T. Kawada, Y. Ikeda, M. Sugimachi, T. Shishido, O. Kawaguchi, T. Yamazaki, J. Alexander Jr., and K. Sunagawa, "Bidirectional augmentation of heart rate regulation by autonomic nervous system in rabbits," *Amer. J. Physiol.*, vol. 271, no. 1, pp. H288–H295, Jul. 1996.

[9] T. Kawada, M. Sugimachi, T. Shishido, H. Miyano, Y. Ikeda, R. Yoshimura, T. Sato, H. Takaki, J. Alexander Jr., and K. Sunagawa, "Dynamic vagosympathetic interaction augments heart rate response irrespective of stimulation patterns," *Amer. J. Physiol.*, vol. 272, no. 5, pp. H2180–H2187, May 1997.

[10] T. Sato, T. Kawada, M. Inagaki, T. Shishido, H. Takaki, M. Sugimachi, and K. Sunagawa, "New analytic framework for understanding sympathetic baroreflex control of arterial pressure," *Amer. J. Physiol.*, vol. 276, no. 6, pp. H2251–H2261, Jun. 1999.

[11] T. Kawada, T. Shishido, M. Inagaki, C. Zheng, Y. Yanagiya, K. Uemura, M. Sugimachi, and K. Sunagawa, "Estimation of baroreflex gain using a baroreflex equilibrium diagram," *Jpn. J. Physiol.*, vol. 52, no. 1, pp. 21–29, Feb. 2002.

[12] T. Sato, T. Kawada, M. Inagaki, T. Shishido, M. Sugimachi, and K. Sunagawa, "Dynamics of sympathetic baroreflex control of arterial pressure in rats," *Amer. J. Physiol.*, vol. 285, no. 1, pp. R262–R270, Jul. 2003.

[13] Y. Ikeda, T. Kawada, M. Sugimachi, O. Kawaguchi, T. Shishido, T. Sato, H. Miyano, W. Matsuura, J. Alexander Jr., and K. Sunagawa, "Neural arc of baroreflex optimizes dynamic pressure regulation in achieving both stability and quickness," *Amer. J. Physiol.*, vol. 271, no. 3, pp. H882–H890, Sep. 1996.

[14] K. Sunagawa, T. Sato, and T. Kawada, "Integrative sympathetic baroreflex regulation of arterial pressure," *Ann. NY Acad. Sci.*, vol. 940, pp. 314–323, Jun. 2001.

[15] A. J. Linenthal, "Quantitative studies in man of the cardiovascular effects of reflex vagal stimulation produced by carotid sinus pressure. I. Localization of an increased effect in a patient with angina pectoris," *Circulation*, vol. 5, no. 1, pp. 81–84, Jan. 1952.

[16] E. Braunwald, S. E. Epstein, G. Glick, A. S. Wechsler, and N. S. Braunwald, "Relief of angina pectoris by electrical stimulation of the carotid-sinus nerves," *New Eng. J. Med.*, vol. 277, no. 24, pp. 1278–1283, Dec. 1967.

[17] S. I. Schwartz, L. S. Griffith, A. Neistadt, and N. Hagfors, "Chronic carotid sinus nerve stimulation in the treatment of essential hypertension," *Amer. J. Surg.*, vol. 114, no. 1, pp. 5–15, Jul. 1967.

[18] Y. Nakayama, H. Miyano, T. Shishido, M. Inagaki, T. Kawada, M. Sugimachi, and K. Sunagawa, "Heart rate-independent vagal effect on end-systolic elastance of the canine left ventricle under various levels of sympathetic tone," *Circulation*, vol. 104, no. 19, pp. 2277–2279, Nov. 2001.

[19] E. Braunwald, S. F. Vatner, N. S. Braunwald, and B. E. Sobel, "Carotid sinus nerve stimulation in the treatment of angina pectoris and supraventricular tachycardia," *Calif. Med.*, vol. 112, no. 3, pp. 41–50, Mar. 1970.

[20] D. T. Mason, J. F. Spann, Jr, R. Zelis, and E. A. Amsterdam, "Physiologic approach to the treatment of angina pectoris," *New Eng. J. Med.*, vol. 281, no. 22, pp. 1225–1228, Nov. 1969.

[21] S. F. Vatner, D. Franklin, R. L. Van Citters, and E. Braunwald, "Effects of carotid sinus nerve stimulation on blood-flow distribution in conscious dogs at rest and during exercise," *Circ. Res.*, vol. 27, no. 4, pp. 495–503, Oct. 1970.

[22] F. Solti, S. Juhász-Nagy, Z. Szabó, M. Iskum, and I. Krasznai, "Effect of the carotid sinus nerve stimulation on nutritive myocardial blood flow in regional cardiac ischaemia," *Basic Res. Cardiol.*, vol. 70, no. 5, pp. 531–536, Sep.-Oct. 1975.

[23] F. Solti and A. Jahász-Nagy, "Effect of carotid sinus nerve stimulation on coronary blood flow in myocardial ischaemia: Role of the collateral vessels," *Basic Res. Cardiol.*, vol. 70, no. 6, pp. 639–646, Nov.-Dec. 1975.

[24] S. E. Epstein, G. D. Beiser, R. E. Goldstein, D. Redwood, D. R. Rosing, G. Glick, A. S. Wechsler, M. Stampfer, L. S. Cohen, R. L. Reis, N. S. Braunwald, and E. Braunwald, "Treatment of angina pectoris by electrical stimulation of the carotid-sinus nerves," *New Eng. J. Med.*, vol. 280, no. 18, pp. 971–978, May 1969.

[25] "Electrical stimulation of the carotid-sinus nerves for angina pectoris," *Lancet*, vol. 294, no. 7616, pp. 362–364, Aug. 1969.

[26] N. S. Braunwald, S. E. Epstein, and E. Braunwald, "Carotid sinus nerve stimulation for the treatment of intractable angina pectoris: Surgical technic," *Ann. Surg.*, vol. 172, no. 5, pp. 870–876, Nov. 1970.

[27] R. Courbier, J. Torresani, J. Houzé, A. Jouve, and E. Henry, "Carotid sinus nerve stimulation in angina pectoris," *J. Cardiovasc. Surg. (Torino)*, vol. 12, no. 3, pp. 231–234, May-Jun. 1971.

[28] H. P. Krayenbühl, W. Meier, and W. Burian, "Die Behandlung der Angina Pectoris Durch elektrische Stimulation der Karotissinusnerven (Treatment of angina pectoris by electric stimulation of the carotid sinus nerves)," (in German) *Schweiz. Med. Wochenschr.*, vol. 102, no. 47, pp. 1739–1741, Nov. 1972.

[29] "Carotid-sinus-nerve electro-stimulation in angina pectoris," *Lancet*, vol. 301, no. 7798, p. 304, Feb. 1973.

[30] J. C. Lopshire, X. Zhou, C. Dusa, T. Ueyama, J. Rosenberger, N. Courtney, M. Ujhelyi, T. Mullen, M. Das, and D. P. Zipes, "Spinal cord stimulation improves ventricular function and reduces ventricular arrhythmias in a canine postinfarction heart failure model," *Circulation*, vol. 120, no. 4, pp. 286–294, Jul. 2009.

[31] G. H. Heidorn and A. P. McNamara, "Effect of carotid sinus stimulation on the electrocardiograms of clinically normal individuals," *Circulation*, vol. 14, no. 6, pp. 1104–1113, Dec. 1956.

[32] B. Lown and S. A. Levine, "The carotid sinus. Clinical value of its stimulation," *Circulation*, vol. 23, pp. 766–789, May 1961.

[33] Y. Zhang, K. A. Mowrey, S. Zhuang, D. W. Wallick, Z. B. Popović, and T. N. Mazgalev, "Optimal ventricular rate slowing during atrial fibrillation by feedback AV nodal-selective vagal stimulation," *Amer. J. Physiol.*, vol. 282, no. 3, pp. H1102–H1110, Mar. 2002.

[34] Y. Zhang, H. Yamada, S. Bibevski, S. Zhuang, K. A. Mowrey, D. W. Wallick, S. Oh, and T. N. Mazgalev, "Chronic atrioventricular nodal vagal stimulation: First evidence for long-term ventricular rate control in canine atrial fibrillation model," *Circulation*, vol. 112, no. 19, pp. 2904–2911, Nov. 2005.

[35] S. Zhuang, Y. Zhang, K. A. Mowrey, J. Li, T. Tabata, D. W. Wallick, Z. B. Popović, R. A. Grimm, A. Natale, and T. N. Mazgalev, "Ventricular rate control by selective vagal stimulation is superior to rhythm regularization by atrioventricular nodal ablation and pacing during atrial fibrillation," *Circulation*, vol. 106, no. 14, pp. 1853–1858, Oct. 2002.

[36] J. P. DiMarco, "Selective vagal stimulation for rate control in atrial fibrillation," *Circulation*, vol. 106, no. 14, pp. 1746–1747, Oct. 2002.

[37] S. H. Hohnloser, K. H. Kuck, and J. Lilienthal, "Rhythm or rate control in atrial fibrillation—Pharmacological intervention in atrial fibrillation (PIAF): A randomised trial," *Lancet*, vol. 356, no. 9244, pp. 1789–1794, Nov. 2000.

[38] S. Bianchi, P. Rossi, A. D. Scala, and L. Kornet, "Endocardial transcatheter stimulation of the AV nodal fat pad: Stabilization of rapid ventricular rate response during atrial fibrillation in left ventricular failure," *J. Cardiovasc. Electrophysiol.*, vol. 20, no. 1, pp. 103–105, Jan. 2009.

[39] B. L. Bufkin, J. D. Puskas, J. Vinten-Johansen, S. T. Shearer, and R. A. Guyton, "Controlled intermittent asystole: Pharmacologic potentiation of vagal-induced asystole," *Ann. Thorac. Surg.*, vol. 66, no. 4, pp. 1185–1190, Oct. 1998.

[40] M. Scanavacca, C. F. Pisani, D. Hachul, S. Lara, C. Hardy, F. Darrieux, I. Trombetta, C. E. Negrão, and E. Sosa, "Selective atrial vagal denervation guided by evoked vagal reflex to treat patients with paroxysmal atrial fibrillation," *Circulation*, vol. 114, no. 9, pp. 876–885, Aug. 2006.

[41] D. Cerati and P. J. Schwartz, "Single cardiac vagal fiber activity, acute myocardial ischemia, and risk for sudden death," *Circ. Res.*, vol. 69, no. 5, pp. 1389–1401, Nov. 1991.

[42] P. J. Schwartz, E. Vanoli, M. Stramba-Badiale, G. M. De Ferrari, G. E. Billman, and R. D. Foreman, "Autonomic mechanisms and sudden death. New insights from analysis of baroreceptor reflexes in conscious dogs with and without a myocardial infarction," *Circulation*, vol. 78, no. 4, pp. 969–979, Oct. 1988.

[43] M. T. La Rovere, J. T. Bigger, Jr, F. I. Marcus, A. Mortara, and P. J. Schwartz, "Baroreflex sensitivity and heart-rate variability in prediction of total cardiac mortality after myocardial infarction," *Lancet*, vol. 351, no. 9101, pp. 478–484, Feb. 1998.

[44] G. Zuanetti, G. M. De Ferrari, S. G. Priori, and P. J. Schwartz, "Protective effect of vagal stimulation on reperfusion arrhythmias in cats," *Circ. Res.*, vol. 61, no. 3, pp. 429–435, Sep. 1987.

[45] M. Ando, R. G. Katare, Y. Kakinuma, D. Zhang, F. Yamasaki, K. Muramoto, and T. Sato, "Efferent vagal nerve stimulation protects heart against ischemia-induced arrhythmias by preserving connexin43 protein," *Circulation*, vol. 112, no. 2, pp. 164–170, Jul. 2005.

[46] L. S. Griffith and S. I. Schwartz, "Reversal of renal hypertension by electrical stimulation of the carotid sinus nerve," *Surgery*, vol. 56, pp. 232–239, Jul. 1964.

[47] A. M. Bilgutay and C. W. Lillehei, "Treatment of hypertension with an implantable electronic device," *J. Amer. Med. Assoc.*, vol. 191, pp. 649–653, Feb. 1965.

[48] A. Carlsten, B. Folkow, G. Grimby, C. A. Hamberger, and O. Thulesius, "Cardiovascular effects of direct stimulation of the carotid sinus nerve in man," *Acta. Physiol. Scand.*, vol. 44, no. 2, pp. 138–145, Nov. 1958.

[49] T. Agishi, J. Temples, and E. C. Peirce 2nd, "Electrical stimulation of the carotid sinus nerve as an experimental treatment of hypertension," *J. Surg. Res.*, vol. 9, no. 5, pp. 305–309, May 1969.

[50] A. N. Brest, L. Wiener, and B. Bachrach, "Bilateral carotid sinus nerve stimulation in the treatment of hypertension," *Amer. J. Cardiol.*, vol. 29, no. 6, pp. 821–825, Jun. 1972.

[51] F. Solti, Z. Szabó, G. Kerkovits, G. Budai, E. Bodor, and I. Kalmár, "Baropacing of the carotid sinus nerve for treatment of "Intractable" hypertension," *Z. Kardiol.*, vol. 64, no. 4, pp. 368–374, Apr. 1975.

[52] T. E. Lohmeier, E. D. Irwin, M. A. Rossing, D. J. Serdar, and R. S. Kieval, "Prolonged activation of the baroreflex produces sustained hypotension," *Hypertension*, vol. 43, no. 2, pp. 306–311, Feb. 2004.

[53] T. E. Lohmeier, T. M. Dwyer, D. A. Hildebrandt, E. D. Irwin, M. A. Rossing, D. J. Serdar, and R. S. Kieval, "Influence of prolonged baroreflex activation on arterial pressure in angiotensin hypertension," *Hypertension*, vol. 46, no. 5, pp. 1194–200, Nov. 2005.

[54] T. E. Lohmeier, A. M. Barrett, and E. D. Irwin, "Prolonged activation of the baroreflex: A viable approach for the treatment of hypertension?," *Curr. Hypertens. Rep.*, vol. 7, no. 3, pp. 193–198, Jun. 2005.

[55] T. E. Lohmeier, D. A. Hildebrandt, T. M. Dwyer, A. M. Barrett, E. D. Irwin, M. A. Rossing, and R. S. Kieval, "Renal denervation does not abolish sustained baroreflex-mediated reductions in arterial pressure," *Hypertension*, vol. 49, no. 2, pp. 373–379, Feb. 2007.

[56] T. E. Lohmeier, T. M. Dwyer, E. D. Irwin, M. A. Rossing, and R. S. Kieval, "Prolonged activation of the baroreflex abolishes obesity-induced hypertension," *Hypertension*, vol. 49, no. 6, pp. 1307–1314, Jun. 2007.

[57] T. E. Lohmeier, D. A. Hildebrandt, T. M. Dwyer, R. Iliescu, E. D. Irwin, A. W. Cates, and M. A. Rossing, "Prolonged activation of the baroreflex decreases arterial pressure even during chronic adrenergic blockade," *Hypertension*, vol. 53, no. 5, pp. 833–838, May 2009.

[58] T. N. Thrasher, "Unloading arterial baroreceptors causes neurogenic hypertension," *Amer. J. Physiol.*, vol. 282, no. 4, pp. R1044–R1053, Apr. 2002.

[59] T. N. Thrasher, "Baroreceptors and the long-term control of blood pressure," *Exp. Physiol.*, vol. 89, no. 4, pp. 331–335, Jul. 2004.

[60] C. J. Dickinson, "Re: Baroreceptors and the long-term control of blood pressure," *Exp. Physiol.*, vol. 89, no. 4, pp. 335–337, Jul. 2004.

[61] P. Sleight, "Arterial baroreflexes can determine long-term blood pressure. Baroreceptors and hypertension: Time for a re-think?," *Exp. Physiol.*, vol. 89, no. 4, pp. 337–341, Jul. 2004.

[62] T. N. Thrasher, "Effects of chronic baroreceptor unloading on blood pressure in the dog," *Amer. J. Physiol.*, vol. 288, no. 4, pp. R863–R871, Apr. 2005.

[63] T. N. Thrasher, "Baroreceptors, baroreceptor unloading, and the long-term control of blood pressure," *Amer. J. Physiol.*, vol. 288, no. 4, pp. R819–R827, Apr. 2005.

[64] T. N. Thrasher, "Arterial baroreceptor input contributes to long-term control of blood pressure," *Curr. Hypertens. Rep.*, vol. 8, no. 3, pp. 249–254, Jun. 2006.

[65] P. A. Munch, M. C. Andresen, and A. M. Brown, "Rapid resetting of aortic baroreceptors in vitro," *Amer. J. Physiol.*, vol. 244, no. 5, pp. H672–H680, May 1983.

[66] H. R. Warner, "The frequency-dependent nature of blood pressure regulation by the carotid sinus studied with an electric analog," *Circ. Res.*, vol. 6, no. 1, pp. 35–40, Jan. 1958.

[67] D. Michikami, A. Kamiya, T. Kawada, M. Inagaki, T. Shishido, K. Yamamoto, H. Ariumi, S. Iwase, J. Sugenoya, K. Sunagawa, and M. Sugimachi, "Short-term electroacupuncture at Zusanli resets the arterial baroreflex neural arc toward lower sympathetic nerve activity," *Amer. J. Physiol.*, vol. 291, no. 1, pp. H318–H326, Jul. 2006.

[68] M. Sugimachi, T. Kawada, H. Yamamoto, A. Kamiya, T. Miyamoto, and K. Sunagawa, "Modification of autonomic balance by electrical acupuncture does not affect baroreflex dynamic characteristics," in *Conf. Proc. IEEE Eng. Med. Biol. Soc.*, 2008, vol. 2008, pp. 1981–1984.

[69] T. Kawada, S. Shimizu, H. Yamamoto, T. Shishido, A. Kamiya, T. Miyamoto, K. Sunagawa, and M. Sugimachi, "Servo-controlled hind-limb electrical stimulation for short-term arterial pressure control," *Circ. J.*, vol. 73, no. 5, pp. 851–859, May 2009.

[70] H. Yamamoto, T. Kawada, A. Kamiya, T. Kita, and M. Sugimachi, "Electroacupuncture changes the relationship between cardiac and renal sympathetic nerve activities in anesthetized cats," *Auton. Neurosci.*, vol. 144, no. 1-2, pp. 43–49, Dec. 2008.

[71] Y. Yanagiya, T. Sato, T. Kawada, M. Inagaki, T. Tatewaki, C. Zheng, A. Kamiya, H. Takaki, M. Sugimachi, and K. Sunagawa, "Bionic epidural stimulation restores arterial pressure regulation during orthostasis," *J. Appl. Physiol.*, vol. 97, no. 3, pp. 984–990, Sep. 2004.

[72] F. Yamasaki, T. Ushida, T. Yokoyama, M. Ando, K. Yamashita, and T. Sato, "Artificial baroreflex: Clinical application of a bionic baroreflex system," *Circulation*, vol. 113, no. 5, pp. 634–639, Feb. 2006.

[73] K. Yamamoto, T. Kawada, A. Kamiya, H. Takaki, T. Shishido, K. Sunagawa, and M. Sugimachi, "Muscle mechanoreflex augments arterial baroreflex-mediated dynamic sympathetic response to carotid sinus pressure," *Amer. J. Physiol.*, vol. 295, no. 3, pp. H1081–H1089, Sep. 2008.

[74] K. Yamamoto, T. Kawada, A. Kamiya, H. Takaki, M. Sugimachi, and K. Sunagawa, "Static interaction between muscle mechanoreflex and arterial baroreflex in determining efferent sympathetic nerve activity," *Amer. J. Physiol.*, vol. 289, no. 4, pp. H1604–H1609, Oct. 2005.

[75] K. Yamamoto, T. Kawada, A. Kamiya, H. Takaki, T. Miyamoto, M. Sugimachi, and K. Sunagawa, "Muscle mechanoreflex induces the pressor response by resetting the arterial baroreflex neural arc," *Amer. J. Physiol.*, vol. 286, no. 4, pp. H1382–H1388, Apr. 2004.

[76] M. Yoshida, Y. Murayama, A. Chishaki, and K. Sunagawa, "Noninvasive transcutaneous bionic baroreflex system prevents severe orthostatic hypotension in patients with spinal cord injury," in *Conf. Proc. IEEE Eng. Med. Biol. Soc.*, 2008, vol. 2008, pp. 1985–1987.

[77] J. N. Townend and W. A. Littler, "Cardiac vagal activity: A target for intervention in heart disease," *Lancet*, vol. 345, no. 8955, pp. 937–938, Apr. 1995.

[78] M. Li, C. Zheng, T. Sato, T. Kawada, M. Sugimachi, and K. Sunagawa, "Vagal nerve stimulation markedly improves long-term survival after chronic heart failure in rats," *Circulation*, vol. 109, no. 1, pp. 120–124, Jan. 2004.

[79] C. Zheng, M. Li, M. Inagaki, T. Kawada, K. Sunagawa, and M. Sugimachi, "Vagal stimulation markedly suppresses arrhythmias in conscious rats with chronic heart failure after myocardial infarction," in *Conf. Proc. IEEE Eng. Med. Biol. Soc.*, 2005, vol. 7, pp. 7072–7075, 1.

[80] M. Li, C. Zheng, M. Inagaki, T. Kawada, K. Sunagawa, and M. Sugimachi, "Chronic vagal stimulation decreased vasopressin secretion and sodium ingestion in heart failure rats after myocardial infarction," in *Conf. Proc. IEEE Eng. Med. Biol. Soc.*, 2005, vol. 4, pp. 3962–3965.

[81] T. Kawada, T. Yamazaki, T. Akiyama, M. Li, H. Ariumi, H. Mori, K. Sunagawa, and M. Sugimachi, "Vagal stimulation suppresses ischemia-induced myocardial interstitial norepinephrine release," *Life Sci.*, vol. 78, no. 8, pp. 882–887, Jan. 2006.

[82] T. Kawada, T. Yamazaki, T. Akiyama, H. Kitagawa, S. Shimizu, M. Mizuno, M. Li, and M. Sugimachi, "Vagal stimulation suppresses ischemia-induced myocardial interstitial myoglobin release," *Life Sci.*, vol. 83, no. 13-14, pp. 490–495, Sep. 2008.

[83] K. Uemura, M. Li, T. Tsutsumi, T. Yamazaki, T. Kawada, A. Kamiya, M. Inagaki, K. Sunagawa, and M. Sugimachi, "Efferent vagal nerve stimulation induces tissue inhibitor of metalloproteinase-1 in myocardial ischemia-reperfusion injury in rabbit," *Amer. J. Physiol.*, vol. 293, no. 4, pp. H2254–H2261, Oct. 2007.

[84] L. V. Borovikova, S. Ivanova, M. Zhang, H. Yang, G. I. Botchkina, L. R. Watkins, H. Wang, N. Abumrad, J. W. Eaton, and K. J. Tracey, "Vagus nerve stimulation attenuates the systemic inflammatory response to endotoxin," *Nature*, vol. 405, no. 6785, pp. 458–462, May 2000.

[85] K. J. Tracey, "The inflammatory reflex," *Nature*, vol. 420, no. 6917, pp. 853–859, Dec. 2002.

[86] H. Wang, M. Yu, M. Ochani, C. A. Amella, M. Tanovic, S. Susarla, J. H. Li, H. Wang, H. Yang, L. Ulloa, Y. Al-Abed, C. J. Czura, and K. J. Tracey, "Nicotinic acetylcholine receptor alpha7 subunit is an essential regulator of inflammation," *Nature*, vol. 421, no. 6821, pp. 384–388, Jan. 2003.

[87] K. J. Tracey and H. S. Warren, "Human genetics: An inflammatory issue," *Nature*, vol. 429, no. 6987, pp. 35–37, May 2004.

[88] J. Springer, D. O. Okonko, and S. D. Anker, "Vagal nerve stimulation in chronic heart failure: An antiinflammatory intervention?," *Circulation*, vol. 110, no. 4, p. e34, Jul. 2004.

[89] S. Guarini, D. Altavilla, M. M. Cainazzo, D. Giuliani, A. Bigiani, H. Marini, G. Squadrito, L. Minutoli, A. Bertolini, R. Marini, E. B. Adamo, F. S. Venuti, and F. Squadrito, "Efferent vagal fibre stimulation blunts nuclear factor-kappaB activation and protects against hypovolemic hemorrhagic shock," *Circulation*, vol. 107, no. 8, pp. 1189–1194, Mar. 2003.

[90] G. M. De Ferrari, A. Sanzo, H. J. G. M. Crijns, R. Dennert, G. Milasinovic, S. Raspopovic, M. Borggrefe, C. Wolpert, J. Kuschyk, A. Schoene, H. Klein, J. Smid, A. Gavazzi, M. Zabel, and P. J. Schwartz, *Chronic Vagus Nerve Stimulation: A New Treatment Modality for Congestive Heart Failure.* Orlando, FL: American College of Cardiology, 2009.

[91] I. H. Zucker, J. F. Hackley, K. G. Cornish, B. A. Hiser, N. R. Anderson, R. Kieval, E. D. Irwin, D. J. Serdar, J. D. Peuler, and M. A. Rossing, "Chronic baroreceptor activation enhances survival in dogs with pacing-induced heart failure," *Hypertension*, vol. 50, no. 5, pp. 904–910, Nov. 2007.

[92] G. I. Voss, P. G. Katona, and H. J. Chizeck, "Adaptive multivariable drug delivery: Control of arterial pressure and cardiac output in anesthetized dogs," *IEEE Trans. Biomed. Eng.*, vol. BE-34, pp. 617–623, Aug. 1987.

[93] C. Yu, P. J. Roy, H. Kaufman, and B. W. Bequette, "Multiple-model adaptive predictive control of mean arterial pressure and cardiac output," *IEEE Trans. Biomed. Eng.*, vol. 39, pp. 765–778, Aug. 1992.
[94] K. Uemura, M. Sugimachi, T. Kawada, A. Kamiya, Y. Jin, K. Kashihara, and K. Sunagawa, "A novel framework of circulatory equilibrium," *Amer. J. Physiol.*, vol. 286, no. 6, pp. H2376–H2385, Jun. 2004.
[95] A. C. Guyton, A. W. Lindsey, B. Abernathy, and T. Richardson, "Venous return at various right atrial pressures and the normal venous return curves," *Amer. J. Physiol.*, vol. 189, no. 3, pp. 609–615, Jun. 1957.
[96] K. Sagawa, L. Maughan, H. Suga, and K. Sunagawa, *Cardiac Contraction and the Pressure-Volume Relationship*. New York: Oxford Univ. Press, 1988, ch. 5, pp. 232–298.
[97] K. Uemura, T. Kawada, A. Kamiya, T. Aiba, I. Hidaka, K. Sunagawa, and M. Sugimachi, "Prediction of circulatory equilibrium in response to changes in stressed blood volume," *Amer. J. Physiol.*, vol. 289, no. 1, pp. H301–H307, Jul. 2005.
[98] K. Uemura, A. Kamiya, I. Hidaka, T. Kawada, S. Shimizu, T. Shishido, M. Yoshizawa, M. Sugimachi, and K. Sunagawa, "Automated drug delivery system to control systemic arterial pressure, cardiac output, and left heart filling pressure in acute decompensated heart failure," *J. Appl. Physiol.*, vol. 100, no. 4, pp. 1278–1286, Apr. 2006.
[99] K. Uemura, K. Sunagawa, and M. Sugimachi, "Computationally managed bradycardia improved cardiac energetics while restoring normal hemodynamics in heart failure," *Ann. Biomed. Eng.*, vol. 37, no. 1, pp. 82–93, Jan. 2009.
[100] K. Hayashida, K. Sunagawa, M. Noma, M. Sugimachi, H. Ando, and M. Nakamura, "Mechanical matching of the left ventricle with the arterial system in exercising dogs," *Circ. Res.*, vol. 71, no. 3, pp. 481–489, Sep. 1992.
[101] M. Sugimachi, K. Todaka, K. Sunagawa, and M. Nakamura, "Optimal afterload for the heart vs. optimal heart for the afterload," *Front. Med. Biol. Eng.*, vol. 2, no. 3, pp. 217–221, 1990.

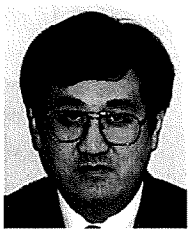

Masaru Sugimachi (A'98–M'06) received the M.D. degree and the Ph.D. degree in biomedical engineering from Kyushu University, Fukuoka, Japan, in 1984 and 1992, respectively.

He is the Director of the Department of Cardiovascular Dynamics, National Cardiovascular Center Research Institute, Osaka, Japan, which he joined in 1992. There, he integrated the research team for the clinical application of bionic cardiology. Since 2004, he has chaired the department. He has published more than 160 original papers in cardiac mechanics, cardiovascular regulation, modeling of biological systems, and bionic medicine. He has been a Principal Investigator of two national research projects (implantable cardiac autonomic neuroregulators, next-generation ICDs) and is currently a Principal Investigator of two other projects (distributed micropacemakers and intensive cardiac care autopilot system).

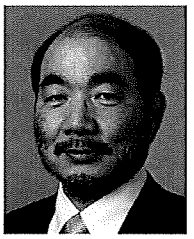

Kenji Sunagawa (M'95–SM'06) received the M.D. degree and the Ph.D. degree in biomedical engineering from Kyushu University, Fukuoka, Japan, in 1974 and 1985, respectively

He is Chairman of and a Professor in the Department of Cardiovascular Medicine, Graduate School of Medical Sciences, Kyushu University. He has been a member of the Administrative Committee of the Japanese Society of Medical Electronics and Biological Engineering. In 1978, he joined the Department of Biomedical Engineering, The Johns Hopkins Medical School, where he established the concept of ventricular-arterial coupling. The coupling concept has been adopted for many textbooks of cardiology and cardiac physiology worldwide. From 1992 to 2004, he chaired the Department of Cardiovascular Dynamics, the National Cardiovascular Center, Osaka, Japan, and developed the basis of bionic cardiology.

Am J Physiol Heart Circ Physiol 297: H53–H58, 2009.
First published May 15, 2009; doi:10.1152/ajpheart.00260.2009.

Slow head-up tilt causes lower activation of muscle sympathetic nerve activity: loading speed dependence of orthostatic sympathetic activation in humans

Atsunori Kamiya,[1,2] Toru Kawada,[1] Shuji Shimizu,[1] Satoshi Iwase,[2,3] Masaru Sugimachi,[1] and Tadaaki Mano[2,4]

[1]*Department of Cardiovascular Dynamics, National Cardiovascular Center Research Institute, Suita;* [2]*Research Institute of Environmental Medicine, Nagoya University, Nagoya;* [3]*Department of Physiology, Aichi Medical University, Aichi; and* [4]*Gifu University of Medical Science, Gifu, Japan*

Submitted 17 March 2009; accepted in final form 13 May 2009

Kamiya A, Kawada T, Shimizu S, Iwase S, Sugimachi M, Mano T. Slow head-up tilt causes lower activation of muscle sympathetic nerve activity: loading speed dependence of orthostatic sympathetic activation in humans. *Am J Physiol Heart Circ Physiol* 297: H53–H58, 2009. First published May 15, 2009; doi:10.1152/ajpheart.00260.2009.—Many earlier human studies have reported that increasing the tilt angle of head-up tilt (HUT) results in greater muscle sympathetic nerve activity (MSNA) response, indicating the amplitude dependence of sympathetic activation in response to orthostatic stress. However, little is known about whether and how the inclining speed of HUT influences the MSNA response to HUT, independent of the magnitude of HUT. Twelve healthy subjects participated in passive 30° HUT tests at inclining speeds of 1° (control), 0.1° (slow), and 0.0167° (very slow) per second. We recorded MSNA (tibial nerve) by microneurography and assessed nonstationary time-dependent changes of R-R interval variability using a complex demodulation technique. MSNA averaged over every 10° tilt angle increased during inclination from 0° to 30°, with smaller increases in the slow and very slow tests than in the control test. Although a 3-min MSNA overshoot after reaching 30° HUT was observed in the control test, no overshoot was detected in the slow and very slow tests. In contrast with MSNA, increases in heart rate during the inclination and after reaching 30° were similar in these tests, probably because when compared with the control test, greater increases in plasma epinephrine counteracted smaller autonomic responses in the very slow test. These results indicate that slower HUT results in lower activation of MSNA, suggesting that HUT-induced sympathetic activation depends partially on the speed of inclination during HUT in humans.

autonomic nervous system; baroreflex; heart rate variability; microneurography

HUMANS HAVE BEEN SUBJECTED to ceaseless orthostatic stresses since they first evolved and assume an orthostatic posture most of their lives. Thus the maintenance of arterial pressure (AP) under orthostatic stress against gravity-driven fluid shift is of great importance. During standing, gravitational fluid shift toward the lower part of the body (i.e., abdominal vascular bed, lower limbs) would cause severe orthostatic hypotension if not counteracted by compensatory mechanisms (27). Orthostatic sympathetic activation mediated by arterial baroreflex has been considered to be the major compensatory mechanism (2, 26, 27) since denervation of baroreceptor afferents causes profound postural hypotension (30). Therefore, many earlier human studies have recorded muscle sympathetic nerve activity (MSNA) by microneurographic technique and investigated MSNA response to various orthostatic stresses such as head-up tilt (HUT) and lower body negative pressure (LBNP) (1, 5, 24). One of the important findings is that stronger orthostatic stress results in greater MSNA response during incremental HUT (3, 13, 14, 28) and LBNP (17), indicating the amplitude dependence of orthostatic MSNA activation. However, less attention has been paid to the effects of loading speed of orthostatic stress on orthostatic sympathetic activation in humans. Although earlier studies reported that rapid HUT causes dynamic and transient hemodynamic response (33, 34, 36), they did not investigate MSNA. Thus it remains unclear whether and how the inclining speed of HUT affects HUT-induced activation of MSNA (loading speed dependence of orthostatic MSNA activation), independent of the magnitude of HUT. This is an important clinical issue because the speed of upright tilting of each patient's bed would influence his/her autonomic nervous and hemodynamic conditions.

Orthostatic sympathetic activation is mainly mediated by arterial baroreflex control of MSNA, which exhibits high-pass filter dynamic transfer characteristics at least in anesthetized animals such as rabbits (15) and rats (29), indicating that more rapid change of AP results in greater response of MSNA to pressure change (15). Accordingly, we hypothesized that a lower speed of HUT results in less MSNA activation in humans. To test the hypothesis, we performed passive 30° HUT tests at three inclining speeds (1°, 0.1°, and 0.0167°/s) in 12 healthy volunteers. We compared the responses of MSNA measured by microneurography and hemodynamics during these tests.

METHODS

Subjects

The subjects were 12 healthy volunteers (10 males and 2 females) with a mean age (±SE) of 24 ± 5 yr, mean height of 164 ± 11 cm, and mean weight of 58 ± 9 kg. They were carefully screened by medical history, physical examination, complete blood count, blood chemistry analyses, electrocardiogram, and psychological testing. Candidates were excluded if they had evidence of cardiovascular or other disease, smoked tobacco products, took medications, or were obese (body mass index >30 kg/m^2). None of the subjects had experienced spontaneous syncope within the past 5 yr. All had a sedentary lifestyle and were not athletes. All subjects gave informed consent to participate in this study, which was approved by the

Address for reprint requests and other correspondence: A. Kamiya, Dept. of Cardiovascular Dynamics, National Cardiovascular Center Research Institute, 5-7-1 Fujishirodai, Suita, Osaka 565-8565, Japan (e-mail: kamiya@ri.ncvc.go.jp).

Committee of Human Research, Research Institute of Environmental Medicine at Nagoya University.

Measurements

MSNA was measured in our laboratory by the method reported previously (22, 35). Briefly, a tungsten microelectrode (model 26-05-1; Federick Haer and Company, Bowdoinham, ME) was inserted percutaneously into the muscle nerve fascicles of the tibial nerve at the right popliteal fossa without anesthesia. Nerve signals were fed into a preamplifier (Kohno Instruments) with two active band-pass filters set between 500 and 5,000 Hz and were monitored with a loudspeaker. MSNA was identified according to the following discharge characteristics (22, 35): *1*) pulse-synchronous and spontaneous efferent discharges, *2*) afferent activity evoked by tapping of calf muscles but not in response to a gentle skin touch, and *3*) enhanced during phase II of the Valsalva maneuver.

AP was measured continuously using a finger photoplethysmograph (Finapres, Model 2300; Ohmeda, Englewood, CO) at the heart level. Systolic and diastolic AP was measured from the continuous pressure wave. Mean AP was calculated by averaging the pressure within a pulse wave. The finger pressure was confirmed to match intermittent (every minute) brachial AP measured by an automated sphygmomanometer (BP203MII; Nippon Colin, Komaki, Japan). In addition, distance between brachial cuff sensor and carotid sinus was measured in individuals, and AP at the height of carotid sinus level was then calculated by subtracting hydrostatic fluid pressure at each tilt angle from brachial AP. Electrocardiogram (chest lead II) and thermistor respirogram were also recorded continuously. A 20-gauge intravenous catheter was inserted into the antecubital vein in the left forearm to obtain venous blood samples for determination of plasma concentrations of epinephrine, norepinephrine, and arginine vasopressin. Thoracic impedance was measured using an impedance plethysmograph (AI-601G; Nihon Koden) to estimate tilt-induced decreases in thoracic fluid volume (12, 19).

Protocols

We instructed the subjects to refrain from eating for 3 h before the experiments. The experimental room was air-conditioned at a temperature of 26°C. Each subject was requested to remain supine on a tilt table set at 0° horizontally. After the microneurographic MSNA signal was detected and an intravenous catheter was placed, three HUT tests (control, slow, and very slow) were performed on each subject. The three tests were conducted in a random order, with intervals of at least 20 min between tests.

In the control test, the subject remained supine (0°) and rested for at least 20 min. Baseline blood sample was then collected, and baseline recordings of variables including MSNA were done for 10 min. Thereafter, the tilt table was inclined to 30° in a continuous passive manner at a speed of 1°/s. Thus inclination to 30° required 30 s. After reaching 30°, the tilt table was fixed for 8 min. All variables were monitored continuously. After that, a blood sample was again collected.

The slow and very slow tests were performed similarly to the control test except the speed of inclining the tilt table. The tilt table was continuously inclined to 30° at speeds of 0.1 and 0.0167°/s in the slow and very slow tests, respectively. Thus inclination to 30° required 300 s in the slow test and 1,800 s in the very slow test.

These HUT tests were terminated by returning the tilt table to the 0° horizontal position when any of the following incidents was observed: development of presyncope symptoms such as nausea, sweating, yawning, gray out, and dizziness; and progressive reduction in systolic blood pressure to <80 mmHg.

Data Analysis

Full-wave rectified MSNA signals were fed through a resistance-capacitance low-pass filter at a time constant of 0.1 s to obtain the mean voltage neurogram. The signals were then resampled at 200 Hz together with other cardiovascular variables. MSNA bursts were identified, and their areas were calculated using a computer program custom-built by our laboratory. MSNA was expressed as both the rate of integrated activity per minute (burst rate) and the total activity by integrating individual burst area per minute (total MSNA). Since the burst area, and hence also the total MSNA, was dependent on electrode position, they were expressed as arbitrary units (AU) normalized by the individual's baseline values at supine rest (0°) at the first HUT test (the average of total MSNA per minute during the 10 min of supine rest was given 100 AU). The area of each burst during the subsequent HUT tests was normalized to this value.

Time-dependent changes in amplitudes of low frequency (LF; 0.04–0.15 Hz) and high frequency (HF; 0.15–0.35 Hz) components of R-R interval variability were assessed continuously by complex demodulation using a custom-designed computer program (6, 8, 21). The complex demodulation technique is a nonlinear time-domain method of time series analysis suitable for the investigation of nonstationary/unstable oscillations within an assigned frequency band (8, 21). This method provides instantaneous amplitudes and frequencies of the LF and HF components as a function of time (8, 21). The instantaneous amplitude of HF component of R-R interval variability was used as the index of cardiac vagal nerve activity in this study.

Variables except blood data were averaged over every 10 min during 0° supine rest in all HUT tests. The data were averaged over every 10, 100, and 600 s during inclination of the tilt table from 0° to 30° in the control, slow, and very slow HUT tests, respectively, and averaged over every 1 min after reaching 60° HUT position in all HUT tests. In addition, the data were averaged over every 10° tilt angle during the inclining period.

Statistical Analysis

Data are expressed as means ± SE. Repeated-measure ANOVA was used to compare variables among the speed of HUT tests (control, slow, and very slow). When the main effect or interaction term was found to be significant, post hoc comparisons were made using the Sheffe's F procedure. A P value <0.05 was considered statistically significant.

RESULTS

Figure 1 shows the typical MSNA data during the control, slow, and very slow HUT tests in one subject. Although HUT increased MSNA during inclination of the tilt table from 0° to 30° in all three tests, the increase was apparently greater in the control test than in the slow and very slow tests (Fig. 1). Data from all subjects showed that increases in MSNA averaged over tilt angle (every 10° tilt) during inclination were greater in the control test than in the slow and very slow tests (Fig. 2). In the control test, MSNA showed a transient overshoot of 3 min after reaching 30° HUT and then declined gradually to the steady-state level (Fig. 2). In contrast, in the slow and very slow tests, MSNA reached steady-state levels without overshoot (Fig. 2). The steady-state levels were similar among the control, slow, and very slow tests.

Heart rate averaged over tilt angle (every 10° tilt) increased during all HUT tests, with similar increases in all three tests (Fig. 3). Instantaneous frequencies of LF and HF bands for R-R interval variability were 0.09 and 0.25–0.28 Hz, respectively, and were almost constant during all HUT tests. The LF amplitude of R-R interval variability did not change in any tests (Fig. 3). Of note, although the HF amplitude of R-R interval variability decreased during inclination of the tilt table from 0° to 30°, the decrease averaged over tilt angle was smaller in the

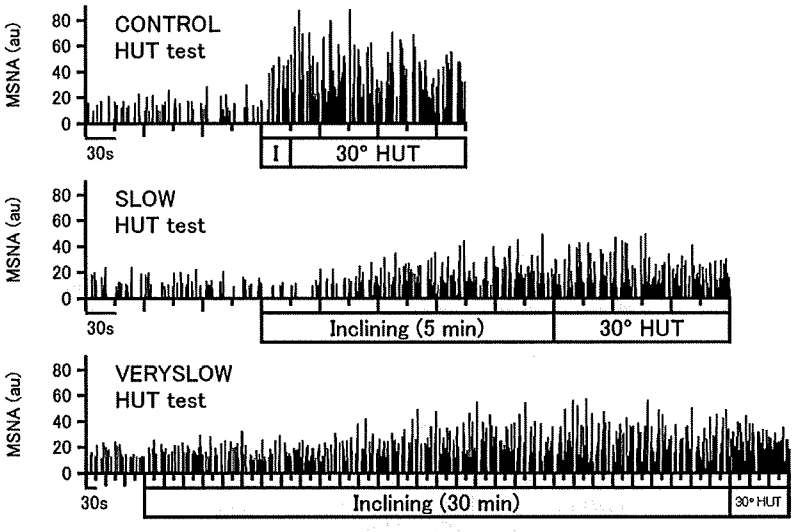

Fig. 1. Representative muscle sympathetic nerve activity (MSNA; integrated signals) data during control (*top*), slow (*middle*), and very slow (*bottom*) head-up tilt (HUT) tests in 1 subject. I (*top*), period of inclination of the tilt bed from 0° supine to 30° HUT posture at an inclining speed of 1°/s. Inclining (*middle* and *bottom*), period of inclination of the tilt bed at speeds of 0.1 and 0.0167°/s, respectively. au, Arbitrary units.

very slow test than in the control and slow tests (Fig. 3). Moreover, the HF amplitude of R-R interval variability reached steady-state levels after reaching 30° HUT, and the level was higher in the very slow test than in the control and slow tests (Fig. 3). Respiratory rate did not change in any tests (Fig. 3).

Systolic AP at the height of brachial level did not change, whereas diastolic AP at the level slightly increased during HUT in the control, slow, and very slow tests. However, there were no differences in both brachial systolic and diastolic APs among the control, slow, and very slow tests (Fig. 4). When AP at the height of carotid sinus level was predicted by subtracting hydrostatic fluid pressure at each tilt angle from brachial AP, systolic and diastolic AP at the carotid sinus level decreased during HUT similarly in the control, slow, and very slow tests (Fig. 4). Thoracic impedance increased during all HUT tests, and the changes averaged over tilt angle were almost identical in all three tests (Fig. 4).

When compared with the 0° supine level, plasma epinephrine concentration increased at the end of HUT tests, with greater increase in the very slow test (from 25.3 ± 3.7 to

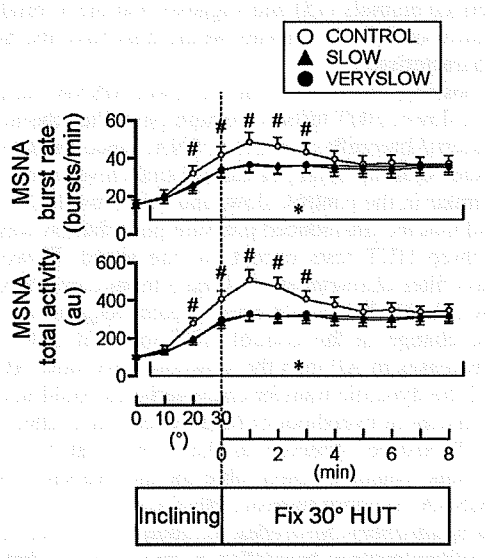

Fig. 2. MSNA burst rate and total activity during control (○), slow (▲), and very slow (●) HUT tests. The *x*-axis to the left of the vertical dotted line indicates that data are averaged over every 10° tilt angle during inclination from 0° supine to 30° HUT, and the *x*-axis to the right of the dotted line indicates that data are averaged over every 1 min after reaching 30° HUT. #$P < 0.05$ vs. slow and very slow tests; *$P < 0.05$ vs. 0° supine. Error bars denote SE.

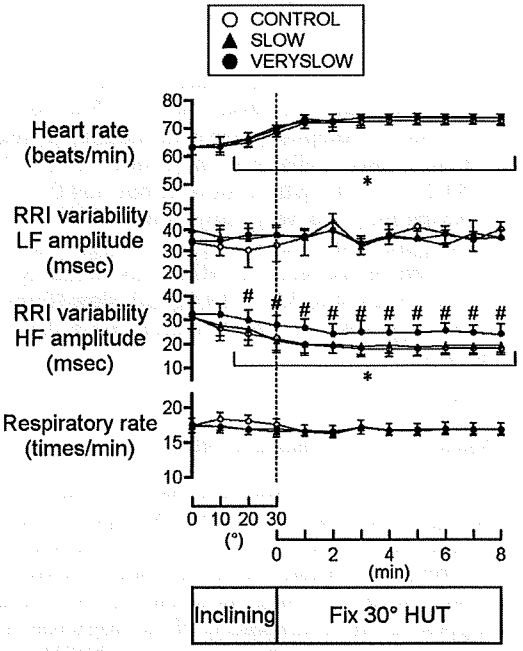

Fig. 3. Heart rate, amplitude of low frequency (LF) and high frequency (HF) component of R-R interval (RRI) variability, and respiratory rate during control (○), slow (▲), and very slow (●) HUT tests. The *x*-axis to the left of the vertical dotted line indicates that data are averaged over every 10° tilt angle during inclination from 0° supine to 30° HUT, and the *x*-axis to the right of the dotted line indicates that data are averaged over every 1 min after reaching 30° HUT. #$P < 0.05$ vs. control and slow tests; *$P < 0.05$ vs. 0° supine posture. Error bars denote SE.

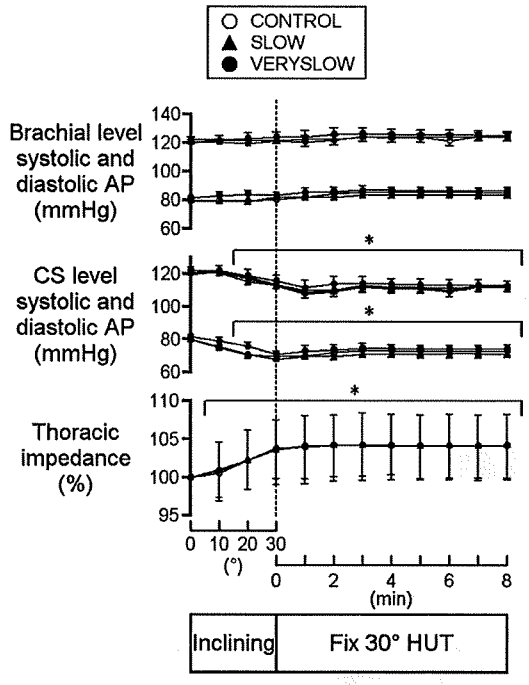

Fig. 4. Systolic and diastolic arterial pressure (AP) measured at the height of brachial level and predicted at the height of carotid sinus (CS) level, and thoracic impedance (percentage of baseline value at 0° supine) during control (○), slow (▲), and very slow (●) HUT tests. The *x*-axis to the left of the vertical dotted line indicates that data are averaged over every 10° tilt angle during inclination from 0° supine to 30° HUT, and the *x*-axis to the right of the dotted line indicates that data are averaged over every 1 min after reaching 30° HUT. *$P < 0.05$ vs. 0° supine posture. Error bars denote SE.

49.3 ± 7.4 pg/ml) than in the control (from 25.8 ± 4.0 to 35.1 ± 5.3 pg/ml) and slow (from 24.3 ± 3.5 to 36.0 ± 5.0 pg/ml) tests. Plasma norepinephrine concentration increased at the end of HUT tests similarly in the control (from 132.2 ± 10.4 to 180.2 ± 11.4 pg/ml), slow (from 134.0 ± 9.2 to 176.5 ± 9.8 pg/ml), and very slow (from 134.2 ± 10.7 to 179.4 ± 9.4 pg/ml) tests. Plasma arginine vasopressin concentration increased at the end of HUT tests similarly in the control (from 3.6 ± 0.4 to 3.9 ± 0.4 pg/ml), slow (from 3.6 ± 0.4 to 3.9 ± 0.4 pg/ml), and very slow (from 3.7 ± 0.4 to 4.0 ± 0.4 pg/ml) tests.

DISCUSSION

Speed Dependence of Orthostatic MSNA Activation

Many earlier human studies have reported that HUT at a larger tilt angle results in greater MSNA response, indicating the amplitude dependence of sympathetic activation in response to orthostatic stress. However, little is known about whether and how the inclining speed during HUT influences MSNA response to HUT, independent of the magnitude of HUT. Our major findings of the present study are that *1*) MSNA averaged over tilt angle increases during inclination of the tilt table from 0° to 30°, with smaller increase in the slow (0.1°/s) and very slow (0.0167°/s) tests than in the control tests (1°/s) and 2) although a 3-min MSNA overshoot after reaching 30° HUT was observed in the control test, no overshoot was found in the slow and very slow tests. These results support our hypothesis that a lower speed of HUT results in less MSNA activation in humans, indicating the loading speed dependence of orthostatic MSNA activation. The speed-dependent sympathetic activation would contribute to prevent hypotension and maintain AP during rapid postural change from supine to upright posture.

Possible Mechanisms for the Speed Dependence of Orthostatic MSNA Activation

Since the HUT activates multiple physiological mechanisms, it is difficult to strictly determine the primary input to humans during postural change from the supine to upright postures. Therefore, we cannot conclude the true mechanisms for the speed dependence of orthostatic MSNA activation observed in this study. In this study, HUT decreased AP at the height of carotid sinus level decreased and increased thoracic impedance. We thus challenged to discuss possible relations of arterial and cardiopulmonary baroreflexes with the speed dependence of orthostatic MSNA activation.

Arterial baroreflex. Although arterial baroreflex is the major mechanism that increases sympathetic nerve activity (SNA) and maintains AP under orthostatic stress (2, 26, 27), it has high-pass filter dynamic transfer characteristics from baroreceptor pressure input to SNA. The high-pass filter characteristics have been investigated in detail by baroreflex open-loop experiments in anesthetized animals such as rabbits (11, 15) and rats (29). This indicates that more rapid change of AP resulted in greater response of SNA to pressure change. In addition, the high-pass filter characteristics might also be observed in earlier human study (10), since MSNA increased/decreased and turned to partially decrease/increase in response to stepwise neck pressure/suction. Although transfer function was not calculated in the study, the SNA response in humans may be consistent with the MSNA response (initial drop and partial recover) to stepwise increase in baroreceptor pressure in anesthetized animals (15) and suggests that the arterial baroreflex control of SNA in humans would also have the high-pass filter characteristics.

One possible mechanism for the lower MSNA during inclination in slower HUT tests is the high-pass filter characteristics of the arterial baroreflex control of SNA. Since the decreases in AP predicted at the height of carotid sinus level over tilt angle were similar in the control, slow, and very slow HUT tests, we assumed that the tilt-induced pressure perturbation was similar in the three HUT tests except for the speed. However, the high-pass filter characteristics of the arterial baroreflex control of SNA (11, 15, 16) would cause greater response of SNA to pressure change in the control HUT test that induced more rapid decreases in AP than the slow and very slow HUT tests. Of note, the dynamic transfer characteristics could not explain a few minutes of overshoot of MSNA activation after reaching 30° HUT posture observed in the control HUT test. Other mechanisms would be responsible for the overshoot of orthostatic MSNA response in faster HUT test.

Cardiopulmonary baroreflex. In addition to arterial baroreflex, cardiopulmonary baroreflex is known to mediate orthostatic activation of SNA. In our results, at a tilt angle of 10°, thoracic impedance increased similarly in control, slow, and very slow tests, indicating that the gravitational fluid shift directed toward the lower part of the body (such as the abdominal vascular bed and lower limbs) may be similar in all

three tests. In addition, MSNA increased at the tilt angle of 10° similarly in control, slow, and very slow tests, but AP predicted at the height of carotid sinus level did not change. These results suggest that cardiopulmonary baroreflex was activated by 10° HUT similarly in these tests and mediated similar magnitude of orthostatic MSNA activation but did not induce speed-dependent differentiation of MSNA. Therefore, it is possible that cardiopulmonary baroreflex control of MSNA does not have high-pass filter characteristics. However, since even small HUT can activate not only cardiopulmonary but also arterial baroreflexes similarly to low levels (i.e., −10 and −15 mmHg) of lower body negative pressure (4), it is difficult to isolate these baroreflexes and to conclude regarding the relation between cardiopulmonary baroreflex and the speed dependence of orthostatic MSNA activation in HUT. In addition, it was reported that cardiopulmonary and arterial baroreceptor afferents interact in a sense of a nonadditive attenuation (25).

Other mechanisms. Mechanisms other than baroreflexes might be responsible for the speed dependence of orthostatic MSNA activation. The first possibility is the vestibulosympathetic reflex, which may be involved in mediating pressor and sympathetic responses to orthostatic stress in rats (23) and humans (31). Since the reflex may be engaged differentially in the control versus the slow and very slow HUT tests, it can relate with the speed dependence of orthostatic MSNA activation observed in this study. The second possibility is the stroke volume, which had a close correlation with MSNA in their changes by orthostatic stress (20), although the neural pathway connecting stroke volume to MSNA may be unclear. Finally, humoral substances can relate with smaller activation of MSNA in the very slow HUT tests. In this study, increases in plasma epinephrine, not norepinephrine and arginine vasopressin, were greater in the very slow test than the control test.

Speed Independence of Orthostatic Tachycardia in the Present Study

In contrast with MSNA, orthostatic tachycardia is independent of inclining speed of HUT. The results may be consistent with a early study (32) that addressed more rapid HUT (i.e., 70° or 90° passive HUT in 3 s, and 70° passive HUT in 1.5 s) and reported that speed of HUT did not affect on initial heart rate responses to rapid HUT. It is difficult to understand the mechanisms for the finding. If baroreflex control of cardiac SNA is similar to that of MSNA as observed in rabbits (15), it is expected that the very slow test mediates a smaller increase in heart rate during inclination than the control test. This raises a possibility that mechanisms other than sympathetic control counteract the speed dependence of orthostatic sympathetic activation and result in speed-independent orthostatic tachycardia. Although we cannot measure cardiac vagal nerve activity in humans, there is a well-known, hypothetical consideration that the HF amplitude of R-R interval variability can reflect respiratory modulation of cardiac vagal nerve activity (7, 9). If so, our results suggest that the decrease in the index of cardiac vagal nerve activity averaged over tilt angle during inclination of HUT was smaller in the very slow HUT test than in the control test (indicating the speed dependence of orthostatic cardiac vagal suppression). Therefore, the speed independence of orthostatic tachycardia in the present study cannot be explained by autonomic neural controls. One possible explanation is that greater increase in plasma epinephrine counteracted the smaller response of sympathetic and, probably, vagal nerve activities.

Limitations

This study has several limitations. First, we used a mild to moderate HUT test (30°) in this study. Sequential HUT tests were necessary for this study, but sequential HUT tests at greater tilt angles (>60°) pose a problem in keeping constant electrode positions for microneurography and maintaining the quality of MSNA recording. Second, since we focused on the effects of slow-speed HUT on orthostatic MSNA response, we used inclining speeds of 1, 0.1, and 0.0167°/s in HUT tests. Finally, the HF amplitude of R-R interval variability is a limited measure of cardiac vagal control in the human (18), although we used it as an index of cardiac vagal modulation in the discussion.

In conclusion, although HUT at an inclining speed of 1°/s causes high MSNA activation with an overshoot of a few minutes, slower HUT (0.1 and 0.0167°/s) results in lower MSNA activation. This indicates that that HUT-induced sympathetic activation depends partially on the tilting speed in humans.

GRANTS

This study was supported by the research project promoted by Ministry of Health, Labour and Welfare in Japan (H18-nano-ippan-003 and H21-nano-ippan-005), the Grants-in-Aid for Scientific Research promoted by Ministry of Education, Culture, Sports, Science and Technology in Japan (20390462), and the Industrial Technology Research Grant Program from New Energy and Industrial Technology Development Organization of Japan (06B44524a).

REFERENCES

1. **Cooke WH, Hoag JB, Crossman AA, Kuusela TA, Tahvanainen KU, Eckberg DL.** Human responses to upright tilt: a window on central autonomic integration. *J Physiol* 517: 617–628, 1999.
2. **Eckberg DL, Sleight P.** *Human baroreflexes in Health and Disease.* New York: Oxford Univ. Press, 1992, p. 3–299.
3. **Fu Q, Okazaki K, Shibata S, Shook RP, Vangunday TB, Galbreath MM, Reelick MF, Levine BD.** Menstrual cycle effects on sympathetic neural responses to upright tilt. *J Physiol* 587: 2019–2031, 2009.
4. **Fu Q, Shibata S, Hastings JL, Prasad A, Palmer MD, Levine BD.** Evidence for unloading arterial baroreceptors during low levels of lower body negative pressure in humans. *Am J Physiol Heart Circ Physiol* 296: H480–H488, 2009.
5. **Furlan R, Porta A, Costa F, Tank J, Baker L, Schiavi R, Robertson D, Malliani A, Mosqueda-Garcia R.** Oscillatory patterns in sympathetic neural discharge and cardiovascular variables during orthostatic stimulus. *Circulation* 101: 886–892, 2000.
6. **Hayano J, Mukai S, Fukuta H, Sakata S, Ohte N, Kimura G.** Postural response of low-frequency component of heart rate variability is an increased risk for mortality in patients with coronary artery disease. *Chest* 120: 1942–1952, 2001.
7. **Hayano J, Sakakibara Y, Yamada A, Yamada M, Mukai S, Fujinami T, Yokoyama K, Watanabe Y, Takata K.** Accuracy of assessment of cardiac vagal tone by heart rate variability in normal subjects. *Am J Cardiol* 67: 199–204, 1991.
8. **Hayano J, Taylor JA, Yamada A, Mukai S, Hori R, Asakawa T, Yokoyama K, Watanabe Y, Takata K, Fujinami T.** Continuous assessment of hemodynamic control by complex demodulation of cardiovascular variability. *Am J Physiol Heart Circ Physiol* 264: H1229–H1238, 1993.
9. **Hayano J, Yasuma F.** Hypothesis: respiratory sinus arrhythmia is an intrinsic resting function of cardiopulmonary system. *Cardiovasc Res* 58: 1–9, 2003.
10. **Ichinose M, Saito M, Kitano A, Hayashi K, Kondo N, Nishiyasu T.** Modulation of arterial baroreflex dynamic response during mild orthostatic stress in humans. *J Physiol* 557: 321–330, 2004.

11. **Ikeda Y, Kawada T, Sugimachi M, Kawaguchi O, Shishido T, Sato T, Miyano H, Matsuura W, Alexander J Jr, Sunagawa K.** Neural arc of baroreflex optimizes dynamic pressure regulation in achieving both stability and quickness. *Am J Physiol Heart Circ Physiol* 271: H882–H890, 1996.
12. **Iwase S, Mano T, Cui J, Kitazawa H, Kamiya A, Miyazaki S, Sugiyama Y, Mukai C, Nagaoka S.** Sympathetic outflow to muscle in humans during short periods of microgravity produced by parabolic flight. *Am J Physiol Regul Integr Comp Physiol* 277: R419–R426, 1999.
13. **Iwase S, Mano T, Watanabe T, Saito M, Kobayashi F.** Age-related changes of sympathetic outflow to muscles in humans. *J Gerontol* 46: M1–M5, 1991.
14. **Kamiya A, Iwase S, Sugiyama Y, Mano T, Sudoh M.** Vasomotor sympathetic nerve activity in men during bed rest and on orthostasis after bed rest. *Aviat Space Environ Med* 71: 142–149, 2000.
15. **Kamiya A, Kawada T, Yamamoto K, Michikami D, Ariumi H, Miyamoto T, Shimizu S, Uemura K, Aiba T, Sunagawa K, Sugimachi M.** Dynamic and static baroreflex control of muscle sympathetic nerve activity (SNA) parallels that of renal and cardiac SNA during physiological change in pressure. *Am J Physiol Heart Circ Physiol* 289: H2641–H2648, 2005.
16. **Kawada T, Zheng C, Yanagiya Y, Uemura K, Miyamoto T, Inagaki M, Shishido T, Sugimachi M, Sunagawa K.** High-cut characteristics of the baroreflex neural arc preserve baroreflex gain against pulsatile pressure. *Am J Physiol Heart Circ Physiol* 282: H1149–H1156, 2002.
17. **Khan MH, Sinoway LI, MacLean DA.** Effects of graded LBNP on MSNA and interstitial norepinephrine. *Am J Physiol Heart Circ Physiol* 283: H2038–H2044, 2002.
18. **Kollai M, Mizsei G.** Respiratory sinus arrhythmia is a limited measure of cardiac parasympathetic control in man. *J Physiol* 424: 329–342, 1990.
19. **Kubicek WG, From AH, Patterson RP, Witsoe DA, Castaneda A, Lillehei RC, Ersek R.** Impedance cardiography as a noninvasive means to monitor cardiac function. *J Assoc Adv Med Instrum* 4: 79–84, 1970.
20. **Levine BD, Pawelczyk JA, Ertl AC, Cox JF, Zuckerman JH, Diedrich A, Biaggioni I, Ray CA, Smith ML, Iwase S, Saito M, Sugiyama Y, Mano T, Zhang R, Iwasaki K, Lane LD, Buckey JC Jr, Cooke WH, Baisch FJ, Eckberg DL, Blomqvist CG.** Human muscle sympathetic neural and haemodynamic responses to tilt following spaceflight. *J Physiol* 538: 331–340, 2002.
21. **Lipsitz LA, Hayano J, Sakata S, Okada A, Morin RJ.** Complex demodulation of cardiorespiratory dynamics preceding vasovagal syncope. *Circulation* 98: 977–983, 1998.
22. **Mano T.** Microneurography as a tool to investigate sympathetic nerve responses to environmental stress. *Aviakosm Ekolog Med* 31: 8–14, 1997.
23. **Matsuda T, Gotoh TM, Tanaka K, Gao S, Morita H.** Vestibulosympathetic reflex mediates the pressor response to hypergravity in conscious rats: contribution of the diencephalon. *Brain Res* 1028: 140–147, 2004.
24. **Mosqueda-Garcia R, Furlan R, Tank J, Fernandez-Violante R.** The elusive pathophysiology of neurally mediated syncope. *Circulation* 102: 2898–2906, 2000.
25. **Persson P, Ehmke H, Kirchheim H, Seller H.** The influence of cardiopulmonary receptors on long-term blood pressure control and plasma renin activity in conscious dogs. *Acta Physiol Scand* 130: 553–561, 1987.
26. **Persson P, Kirchheim H.** *Baroreceptor reflexes: integrative functions and clinical aspects*. Berlin: Springer-Verlag, 1991.
27. **Rowell LB.** *Human cardiovascular control*. New York: Oxford Univ. Press, 1993, p. 3–254.
28. **Saito M, Foldager N, Mano T, Iwase S, Sugiyama Y, Oshima M.** Sympathetic control of hemodynamics during moderate head-up tilt in human subjects. *Environ Med* 41: 151–155, 1997.
29. **Sato T, Kawada T, Inagaki M, Shishido T, Sugimachi M, Sunagawa K.** Dynamics of sympathetic baroreflex control of arterial pressure in rats. *Am J Physiol Regul Integr Comp Physiol* 285: R262–R270, 2003.
30. **Sato T, Kawada T, Sugimachi M, Sunagawa K.** Bionic technology revitalizes native baroreflex function in rats with baroreflex failure. *Circulation* 106: 730–734, 2002.
31. **Sauder CL, Leonard TO, Ray CA.** Greater sensitivity of the vestibulosympathetic reflex in the upright posture in humans. *J Appl Physiol* 105: 65–69, 2008.
32. **Sprangers RL, Veerman DP, Karemaker JM, Wieling W.** Initial circulatory responses to changes in posture: influence of the angle and speed of tilt. *Clin Physiol* 11: 211–220, 1991.
33. **Sundkvist G, Lilja B.** Effect of the degree and speed of tilt on the immediate heart rate reaction. *Clin Physiol* 3: 381–386, 1983.
34. **Toska K, Walloe L.** Dynamic time course of hemodynamic responses after passive head-up tilt and tilt back to supine position. *J Appl Physiol* 92: 1671–1676, 2002.
35. **Wallin BG, Fagius J.** Peripheral sympathetic neural activity in conscious humans. *Annu Rev Physiol* 50: 565–576, 1988.
36. **Wong BJ, Sheriff DD.** Myogenic origin of the hypotension induced by rapid changes in posture in awake dogs following autonomic blockade. *J Appl Physiol* 105: 1837–1844, 2008.

Am J Physiol Heart Circ Physiol 296: H1666–H1674, 2009.
First published February 27, 2009; doi:10.1152/ajpheart.01041.2008.

Angiotensin II disproportionally attenuates dynamic vagal and sympathetic heart rate controls

Toru Kawada,[1] Masaki Mizuno,[1] Shuji Shimizu,[2] Kazunori Uemura,[1] Atsunori Kamiya,[1] and Masaru Sugimachi[1]

[1]*Department of Cardiovascular Dynamics, Advanced Medical Engineering Center, National Cardiovascular Center Research Institute, Osaka and* [2]*Japan Association for the Advancement of Medical Equipment, Tokyo, Japan*

Submitted 29 September 2008; accepted in final form 25 February 2009

Kawada T, Mizuno M, Shimizu S, Uemura K, Kamiya A, Sugimachi M. Angiotensin II disproportionally attenuates dynamic vagal and sympathetic heart rate controls. *Am J Physiol Heart Circ Physiol* 296: H1666–H1674, 2009. First published February 27, 2009; doi:10.1152/ajpheart.01041.2008.—To better understand the pathophysiological role of angiotensin II (ANG II) in the dynamic autonomic regulation of heart rate (HR), we examined the effects of intravenous administration of ANG II (10 $\mu g \cdot kg^{-1} \cdot h^{-1}$) on the transfer function from vagal or sympathetic nerve stimulation to HR in anesthetized rabbits with sinoaortic denervation and vagotomy. In the vagal stimulation group ($n = 7$), we stimulated the right vagal nerve for 10 min using binary white noise (0–10 Hz). The transfer function from vagal stimulation to HR approximated a first-order low-pass filter with pure delay. ANG II attenuated the dynamic gain from 7.6 ± 0.9 to 5.8 ± 0.9 beats·$min^{-1} \cdot Hz^{-1}$ (means ± SD; $P < 0.01$) without affecting the corner frequency or pure delay. In the sympathetic stimulation group ($n = 7$), we stimulated the right postganglionic cardiac sympathetic nerve for 20 min using binary white noise (0–5 Hz). The transfer function from sympathetic stimulation to HR approximated a second-order low-pass filter with pure delay. ANG II slightly attenuated the dynamic gain from 10.8 ± 2.6 to 10.2 ± 3.1 beats·$min^{-1} \cdot Hz^{-1}$ ($P = 0.049$) without affecting the natural frequency, damping ratio, or pure delay. The disproportional suppression of the dynamic vagal and sympathetic regulation of HR would result in a relative sympathetic predominance in the presence of ANG II. The reduced high-frequency component of HR variability in patients with cardiovascular diseases, such as myocardial infarction and heart failure, may be explained in part by the peripheral effects of ANG II on the dynamic autonomic regulation of HR.

systems analysis; transfer function; heart rate variability; cardiac sympathetic nerve activity; rabbit

AUTONOMIC NERVOUS ACTIVITY changes dynamically during daily activity, and thus the dynamic heart rate (HR) regulation by the autonomic nervous system is physiologically important. The high-frequency (HF) component of HR variability (HRV) is thought to reflect primarily vagal nerve activity, because the vagal nerve can change the HR more quickly than the sympathetic nerve (1, 3, 14, 34). This does not mean, however, that the sympathetic system cannot affect the HF component. For example, an increase in background sympathetic tone augments the HR response to vagal stimulation, an effect that has been referred to as accentuated antagonism (20). In accordance with accentuated antagonism, selective cardiac sympathetic nerve stimulation augments the dynamic HR response to vagal stimulation (14). On the other hand, high plasma concentration of norepinephrine (NE) with no direct activation of the cardiac sympathetic nerve attenuates the dynamic HR response to vagal stimulation via an α-adrenergic mechanism (24). These results suggest that the sympathetic system can influence the HF component via complex interactions with the vagal system.

During systemic sympathetic activation, the renin-angiotensin system is activated through stimulation of β_1-adrenergic receptors on juxtaglomerular granular cells (8, 12). In such conditions as hypertension, myocardial ischemia, and heart failure, the renin-angiotensin system and the sympathetic nervous system are both activated (9, 35). Previous studies demonstrated that acute intravenous or intracerebroventricular administration (32) or chronic intravenous administration of angiotensin II (ANG II) modified the baroreflex control of HR in rabbits (5), possibly via a decrease in vagal tone and an increase in sympathetic tone to the heart. In the present study, we focused on the peripheral effects of ANG II and examined the effects of intravenous ANG II on the dynamic HR response to vagal or postganglionic cardiac sympathetic nerve stimulation. In a previous study from our laboratory where anesthetized cats were used, intravenous ANG II (10 $\mu g \cdot kg^{-1} \cdot h^{-1}$) attenuated myocardial interstitial acetylcholine (ACh) release in response to vagal nerve stimulation (17); therefore, we hypothesized that intravenous ANG II at this dose would attenuate the dynamic HR response to vagal nerve stimulation. On the other hand, a previous study from our laboratory where anesthetized rabbits were used demonstrated that intravenous ANG II at a similar dose of 6 $\mu g \cdot kg^{-1} \cdot h^{-1}$ did not affect the peripheral arc transfer function estimated between renal sympathetic nerve activity and arterial pressure (AP) (13). Accordingly, we hypothesized that intravenous administration of ANG II would not modulate the dynamic sympathetic control of HR significantly. We focused on the relative effects of ANG II on the vagal and sympathetic HR regulations because the balance between vagal and sympathetic nerve activities would be a key to understanding the pathophysiology of several cardiovascular diseases.

MATERIALS AND METHODS

Surgical preparations. Animal care was performed in accordance with *Guideline Principles for the Care and Use of Animals in the Field of Physiological Sciences*, which has been approved by the Physiological Society of Japan. All experimental protocols were reviewed and approved by the Animal Subjects Committee at the National Cardiovascular Center. Twenty-one Japanese white rabbits weighing 2.4–3.4 kg were anesthetized with intravenous injections (2 ml/kg) of a mixture of urethane (250 mg/ml) and α-chloralose (40 mg/ml) and mechanically ventilated with oxygen-enriched room air. A double-lumen catheter was inserted into the right femoral vein, and a supplemental dose of the anesthetics was given continuously (0.5–1.0

Address for reprint requests and other correspondence: T. Kawada, Dept. of Cardiovascular Dynamics, Advanced Medical Engineering Center, National Cardiovascular Center Research Institute, 5-7-1 Fujishirodai, Suita, Osaka 565-8565, Japan (e-mail: torukawa@res.ncvc.go.jp).

$ml \cdot kg^{-1} \cdot h^{-1}$). AP was monitored using a micromanometer catheter (Millar Instruments, Houston, TX) inserted into the right femoral artery. HR was determined from the electrocardiogram using a cardiotachometer. Sinoaortic denervation and vagotomy were performed bilaterally to minimize reflex changes in efferent sympathetic nerve activity. The left and right cardiac sympathetic nerves were exposed using a midline thoracotomy and sectioned (16). In the vagal stimulation group, a pair of bipolar stainless steel wire electrodes was attached to the cardiac end of the sectioned right vagal nerve for stimulation. A pair of stainless steel wire electrodes was attached to the proximal end of the sectioned right cardiac sympathetic nerve for recording efferent cardiac sympathetic nerve activity (CSNA). In the sympathetic stimulation group, a pair of bipolar stainless steel wire electrodes was attached to the cardiac end of the sectioned right sympathetic nerve for stimulation. Efferent CSNA was recorded from the proximal end of the sectioned left cardiac sympathetic nerve. The preamplified nerve signal was band-pass filtered between 150 and 1,000 Hz. The signal was then full-wave rectified and low-pass filtered with a cut-off frequency of 30 Hz to quantify the nerve activity. Both the stimulation and recording electrodes were fixed to the nerve by addition-curing silicone glue (Kwik-Sil; World Precision Instruments, Sarasota, FL). We confirmed that the recorded CSNA was mainly postganglionic by observing the disappearance of CSNA following intravenous administration of hexamethonium bromide (50 mg/kg) at the end of each experiment. The body temperature of the animal was maintained at 38°C with a heating pad throughout the experiment.

Protocols. In the vagal stimulation group ($n = 7$), the stimulation amplitude was adjusted (3–6 V) in each animal to yield a HR decrease of ~50 beats/min at 5-Hz tonic stimulation with a pulse duration of 2 ms. To estimate the transfer function from vagal stimulation to HR, a random vagal stimulus was applied for 10 min by altering the stimulus command every 500 ms at either 0 or 10 Hz according to a binary white noise signal. The input power spectral density was relatively constant up to 1 Hz, which covered the upper frequency range of interest with respect to the vagal transfer function in rabbits (26).

In the sympathetic stimulation group ($n = 7$), the stimulation amplitude was adjusted (1–3 V) in each animal to yield a HR increase of ~50 beats/min at 5-Hz tonic stimulation with a pulse duration of 2 ms. To estimate the transfer function from sympathetic stimulation to HR, a random sympathetic stimulus was applied for 20 min by altering the stimulus command every 2 s at either 0 or 5 Hz according to a binary white noise signal. The input power spectral density was relatively constant up to 0.25 Hz, which covered the upper frequency range of interest with respect to the sympathetic transfer function in rabbits (15).

In both the vagal stimulation and sympathetic stimulation groups, the dynamic HR response to nerve stimulation was first recorded under conditions of continuous intravenous infusion of physiological saline solution (1 $ml \cdot kg^{-1} \cdot h^{-1}$). After the control data were recorded, nerve stimulation was stopped and ANG II was intravenously administered at 10 $\mu g \cdot kg^{-1} \cdot h^{-1}$ (1 $ml \cdot kg^{-1} \cdot h^{-1}$ of 10 $\mu g/ml$ solution) instead of the physiological saline solution. After 15 min, we repeated the random stimulation of the vagal or sympathetic nerve while continuing the intravenous injection of ANG II. We used the same binary white noise sequence for the control and ANG II conditions in each animal and changed the sequence for different animals.

In a supplemental protocol ($n = 7$), we examined the time effect on the estimation of the sympathetic transfer function. The 20-min random sympathetic stimulation was repeated twice with an intervening interval of more than 20 min.

Data analysis. Data were digitized at 200 Hz using a 16-bit analog-to-digital converter and stored on the hard disk of a dedicated laboratory computer system. Prestimulation values of HR, AP, and CSNA were calculated by averaging data obtained during the 10 s immediately before nerve stimulation. The mean HR and AP values in response to nerve stimulation were calculated by averaging data obtained during the nerve stimulation period. The mean level of CSNA during the nerve stimulation period was not evaluated because contamination from stimulation artifacts could not be completely eliminated.

The transfer function from nerve stimulation to the HR response was estimated as follows. The input-output data pairs of nerve stimulation and HR were resampled at 10 Hz. To avoid the initial transition from no stimulation to random stimulation biased the transfer function estimation, data were processed only from 2 min after the initiation of random stimulation. In the vagal stimulation group, the data were divided into eight segments of 1,024 data points that half-overlapped with neighboring segments. In the sympathetic stimulation group, the data were divided into eight segments of 2,048 data points that half-overlapped with neighboring segments. For each segment, a linear trend was subtracted and a Hanning window was applied. We then performed a fast Fourier transformation to obtain the frequency spectra of the stimulation command [$X(f)$] and HR [$HR(f)$] (4). We calculated ensemble averages of the power spectral densities of the stimulation command [$S_{X \cdot X}(f)$] and HR [$S_{HR \cdot HR}(f)$] and the cross spectral density between the two signals [$S_{HR \cdot X}(f)$]. Finally, we obtained the transfer function [$H(f)$] from the nerve stimulation to HR response using the following equation (23):

$$H(f) = \frac{S_{HR \cdot X}(f)}{S_{X \cdot X}(f)}$$

To quantify the linear dependence of the HR response to vagal or sympathetic nerve stimulation, we estimated the magnitude-squared coherence function [$Coh(f)$] using the following equation (23):

$$Coh(f) = \frac{|S_{HR \cdot X}(f)|^2}{S_{X \cdot X}(f) \cdot S_{HR \cdot HR}(f)}$$

The coherence function ranges zero and unity and indicates a frequency-domain measure of linear dependence between input and output variables.

Because previous studies found that the transfer function from vagal stimulation to HR approximated a first-order low-pass filter with pure delay (14, 24), we determined the parameters of the vagal transfer function using the following model:

$$H_{vagus}(f) = -\frac{K}{1 + \frac{f}{f_C} j} e^{-2\pi f j L}$$

where K is dynamic gain (in $beats \cdot min^{-1} \cdot Hz^{-1}$), f_C is the corner frequency (in Hz), and L is pure delay (in s). Variables f and j represent frequency and an imaginary unit, respectively. The minus sign in the right side of the equation corresponds to the negative HR response to vagal stimulation.

Because previous studies suggested that the transfer function from sympathetic stimulation to HR approximated a second-order low-pass filter with pure delay (14, 28), we determined the parameters of the sympathetic transfer function using the following model:

$$H_{symp}(f) = \frac{K}{1 + 2\zeta \frac{f}{f_N} j + \left(\frac{f}{f_N} j\right)^2} e^{-2\pi f j L}$$

where K is dynamic gain (in $beats \cdot min^{-1} \cdot Hz^{-1}$), f_N is the natural frequency (in Hz), ζ is the damping ratio, and L is pure delay (in s).

Because deviation of the model transfer function [$H_{model}(f)$] from the estimated transfer function [$H_{est}(f)$] would affect the transfer function parameters, we assessed the goodness of fit using the following equation:

$$\text{Goodness of Fit (\%)} = 100 \times \left[1 - \left(\sum_{m=1}^{N} \frac{|H_{model}(f) - H_{est}(f)|^2}{m}\right) \Big/ \left(\sum_{m=1}^{N} \frac{|H_{est}(f)|^2}{m}\right)\right]$$

$$f = f_0 \times m$$

where f_0, m, and N represent the fundamental frequency of the Fourier transformation, a frequency index, and the number of data points used for the fitting, respectively. When $H_{model}(f)$ is zero for all of the frequencies, the goodness of fit is zero. When $H_{model}(f)$ equals $H_{est}(f)$ for all of the frequencies, the goodness of fit is 100%.

To facilitate intuitive understanding of the dynamic characteristics described by the transfer function (see Appendix A for details), we calculated the step response from the corresponding transfer function as follows. An impulse response of the system was calculated using the inverse Fourier transformation of the estimated transfer function. The step response was then obtained from the time integral of the impulse response. The steady-state response was calculated by averaging the last 10 s of data from the step response. The 80% rise time for the sympathetic step response or the 80% fall time for the vagal step response was estimated as the time at which the step response reached 80% of the steady-state response.

Statistics. All data are presented as means and SD values. Mean values of HR, AP, and CSNA as well as parameters of the transfer functions and step responses were compared between the control and ANG II conditions using paired *t*-tests. Differences were considered significant when $P < 0.05$ (11).

RESULTS

Typical recordings of the vagal stimulation command, HR, and AP obtained under control and ANG II conditions are shown in Fig. 1*A*. The random vagal stimulation began at 60 s. The HR decreased in response to the random vagal stimulation. ANG II, which did not affect the prestimulation baseline HR, attenuated the magnitude of the vagal stimulation-induced variations in HR. ANG II increased the AP both before and during the vagal stimulation. ANG II did not change the prestimulation or poststimulation CSNA (Fig. 1*B*).

As shown in Table 1, ANG II did not affect the mean HR before stimulation of the vagal nerve, whereas it significantly increased the mean HR during the vagal stimulation period. ANG II attenuated the reduction in HR, which was calculated as the difference between the prestimulation HR and the mean HR observed during the vagal stimulation period. ANG II significantly increased the mean AP both before and during the vagal stimulation period. ANG II did not affect the mean level of pre- or poststimulation CSNA significantly.

Figure 2*A* illustrates the averaged transfer functions from vagal stimulation to HR obtained under the control and ANG II conditions. In the gain plots, the transfer gain was relatively constant for frequencies below 0.1 Hz and decreased as the frequency increased above 0.1 Hz. ANG II decreased the transfer gain for all of the investigated frequencies, resulting in

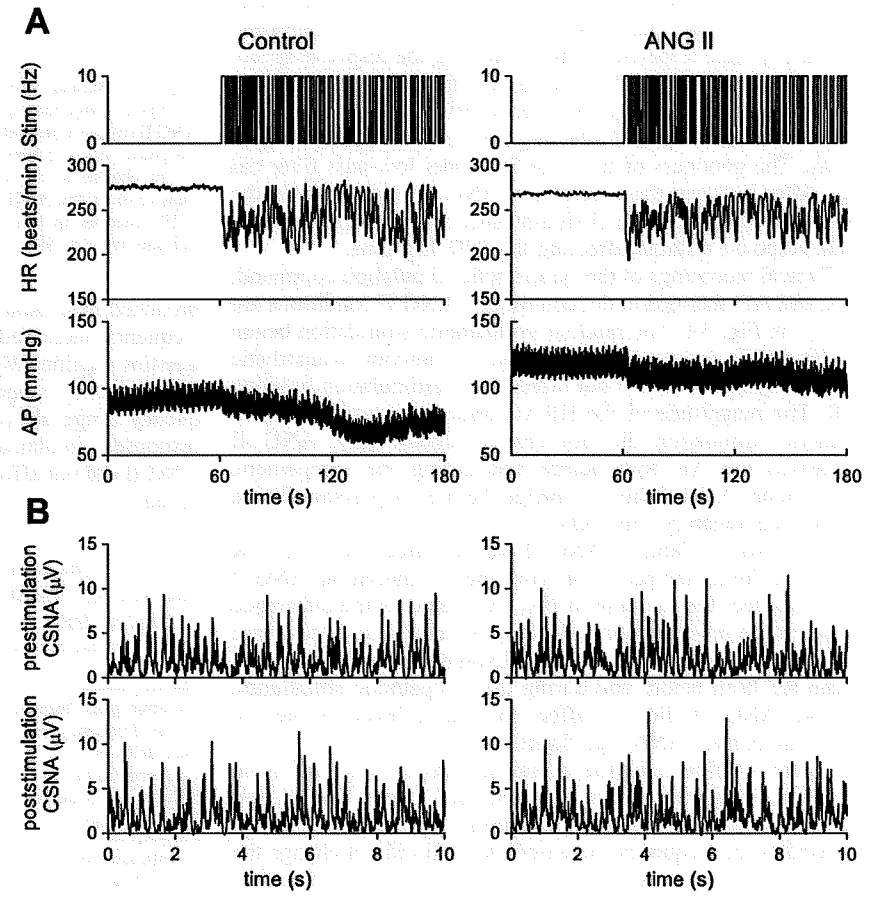

Fig. 1. *A*: representative recordings of vagal nerve stimulation (Stim), the heart rate (HR), and arterial pressure (AP). The *left* and *right* panels show recordings obtained before and during intravenous administration of angiotensin II (ANG II; 10 $\mu g \cdot kg^{-1} \cdot h^{-1}$), respectively. The amplitude of the HR variation in response to vagal stimulation was smaller in the presence of ANG II compared with results obtained without ANG II. *B*: representative recordings of cardiac sympathetic nerve activity (CSNA) under prestimulation baseline and poststimulation conditions. ANG II did not affect the CSNA significantly.

Table 1. *Mean values for HR, AP, and CSNA obtained using the vagal stimulation protocol*

	Control	ANG II	*P* Value
HR, beats/min			
Prestimulation	278±21	281±31	0.60
During stimulation	232±19	245±26*	0.046
Difference‡	−46±6	−37±10†	0.0017
AP, mmHg			
Prestimulation	91±23	127±17†	0.0057
During stimulation	85±24	118±19†	0.0055
Difference‡	−6.3±9.2	−9.2±8.6	0.34
CSNA, μV			
Prestimulation	1.21±0.38 (100%)	1.19±0.46 (98±15%)	0.82
Poststimulation	1.27±0.42 (105±8%)	1.20±0.55 (98±27%)	0.59

Data are means ± SD values; $n = 7$. HR, heart rate; AP, arterial pressure; CSNA, cardiac sympathetic nerve activity. ‡The difference was calculated by subtracting the prestimulation value from the value obtained during the vagal stimulation period in each animal. *$P < 0.05$ and †$P < 0.01$ based on a paired *t*-test. Exact *P* values are also shown.

a parallel downward shift in the gain plot. In the phase plots, the phase approached $-\pi$ radians at 0.01 Hz and the lag became larger as the frequency increased. ANG II did not alter the phase characteristics significantly. In the coherence plots, the coherence value was close to unity in the frequency range from 0.01 to 0.8 Hz. The sharp variation around 0.6 Hz corresponds to the frequency of the artificial ventilation. Figure 2*B* depicts the HR step responses calculated from the corresponding transfer functions. ANG II significantly attenuated the steady-state response without affecting the response speed.

As shown in Table 2, ANG II significantly attenuated the dynamic gain of the vagal transfer function to 76.1 ± 8.5% of the control value without affecting the corner frequency or pure delay. The goodness of fit to the first-order low-pass filter did not differ between the control and ANG II conditions. In the HR step response, ANG II significantly attenuated the steady-state response without affecting the 80% fall time.

Typical recordings of the sympathetic stimulation command, HR, and AP obtained under control and ANG II conditions are shown in Fig. 3*A*. The random sympathetic stimulation began at 60 s. HR increased in response to random sympathetic stimulation. ANG II did not affect the prestimulation baseline HR. The magnitude of the HR variation in response to sympathetic stimulation did not change significantly. ANG II increased the AP both before and during the sympathetic stimulation. ANG II did not change the pre- or poststimulation CSNA significantly (Fig. 3*B*).

As shown in Table 3, ANG II did not affect the mean HR before or during the period of sympathetic stimulation. ANG II did not affect the increase in HR, calculated as the difference between the prestimulation HR and the mean HR in response to sympathetic stimulation. ANG II significantly increased the mean AP both before and during the sympathetic stimulation period. ANG II did not affect the mean level of pre- or poststimulation CSNA significantly.

Figure 4*A* illustrates the averaged transfer functions from sympathetic stimulation to HR obtained under control and ANG II conditions. In the gain plots, the transfer gain decreased as the frequency increased. ANG II did not change the transfer gain markedly. In the phase plots, the phase approached zero radians at 0.01 Hz and increasingly lagged as the frequency increased. ANG II did not affect the phase characteristics significantly. The coherence value was above 0.9 for the frequency range below 0.1 Hz and decreased in the frequency range above 0.1 Hz. Figure 4*B* depicts the HR step responses calculated from the corresponding transfer functions. ANG II did not affect the steady-state response or the response speed.

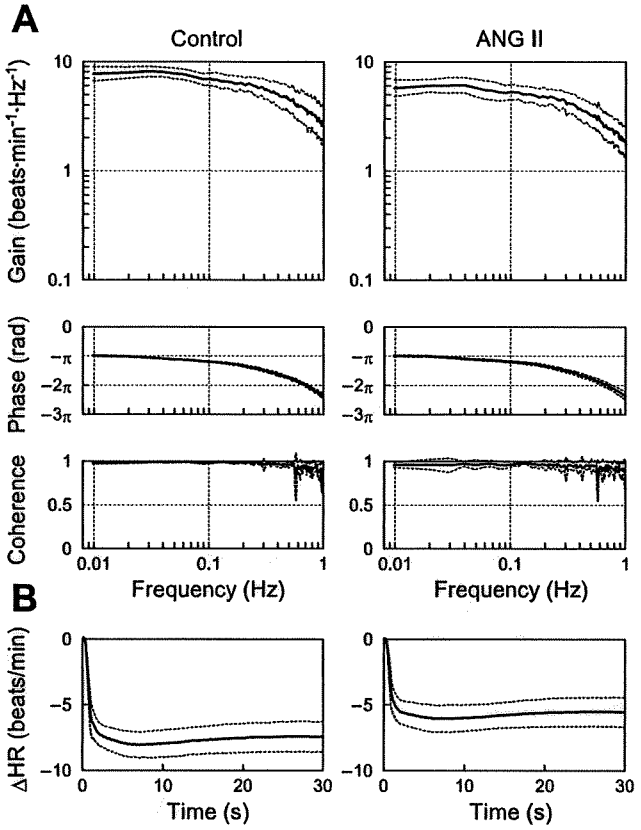

Fig. 2. *A*: averaged transfer functions from vagal nerve stimulation to the HR response obtained before and during intravenous administration of ANG II. Gain plots (*top*), phase plots (*middle*), and coherence plots (*bottom*) are shown. ANG II caused a parallel downward shift in the gain plot. ANG II did not affect the phase plot or coherence plot significantly. *B*: step responses of the HR to a unit change in the vagal stimulation calculated from the corresponding transfer functions. ANG II significantly attenuated the step response of the HR. ΔHR, changes in heart rate. Solid lines indicate mean, and dashed lines indicate mean ± SD.

Table 2. *Effects of ANG II on the parameters of the transfer function and the step response relating to the dynamic vagal control of HR*

	Control	ANG II	*P* Value
Dynamic gain, beats·min^{-1}·Hz^{-1}	7.6±0.9	5.8±0.9*	0.00042
Corner frequency, Hz	0.39±0.12	0.36±0.10	0.12
Pure delay, s	0.48±0.04	0.47±0.06	0.82
Goodness of fit, %	98.8±0.4	98.6±0.8	0.63
Steady-state response, beats/min	−7.4±1.1	−5.6±1.1*	0.0011
80% Fall time	1.31±0.31	1.33±0.37	0.60

Data are means ± SD values; $n = 7$. *$P < 0.01$ based on a paired *t*-test. Exact *P* values are also shown.

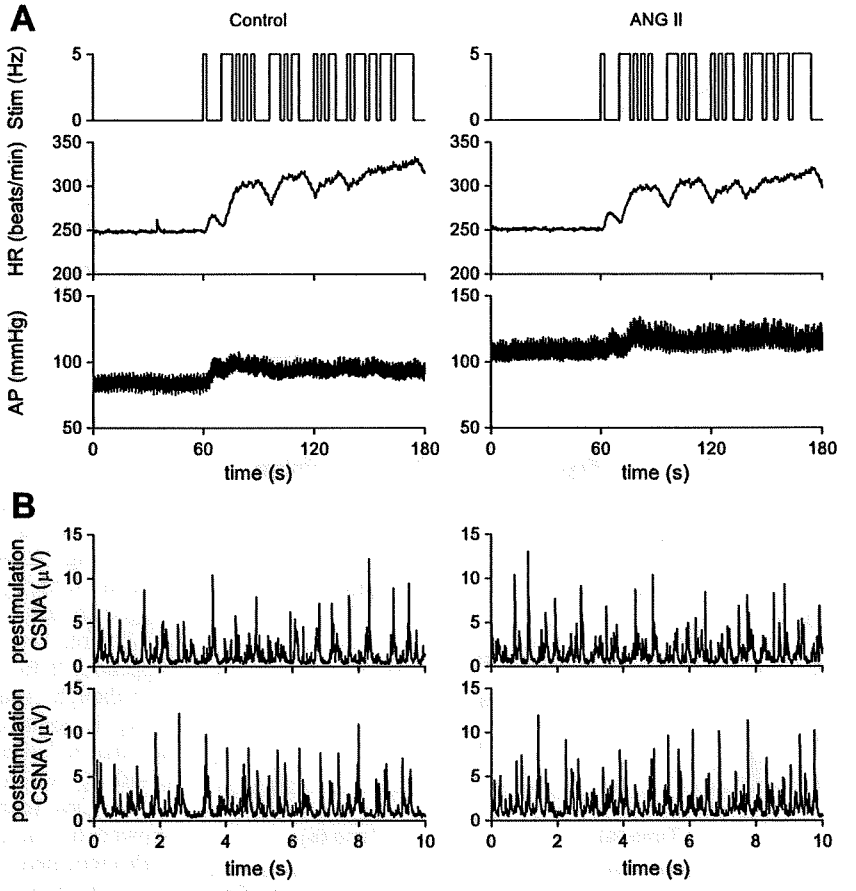

Fig. 3. *A*: representative recordings of cardiac sympathetic nerve stimulation (Stim), HR, and AP. The *left* and *right* panels show the recordings before and during intravenous administration of ANG II (10 $\mu g \cdot kg^{-1} \cdot h^{-1}$), respectively. The amplitude of the HR variation during sympathetic stimulation was unchanged by the addition of ANG II. *B*: representative recordings of CSNA under prestimulation baseline and poststimulation conditions. ANG II did not affect the CSNA significantly.

As shown in Table 4, ANG II slightly attenuated the dynamic gain of the sympathetic transfer function to 92.5 ± 8.9% of the value observed under control conditions. ANG II did not affect the natural frequency, damping ratio, or pure delay. The goodness of fit to the second-order low-pass filter did not differ between the control and ANG II conditions. In the HR step response, ANG II did not affect the steady-state response or the 80% rise time. As shown in Table 5, there were no significant differences in the parameters of the sympathetic transfer function between repeated estimations with an intervening interval of more than 20 min.

Table 3. *Mean values for HR, AP, and CSNA obtained using the sympathetic stimulation protocol*

	Control	ANG II	*P* Value
HR, beats/min			
Prestimulation	267±16	261±19	0.21
During stimulation	317±26	311±23	0.063
Difference†	50±21	50±21	0.94
AP, mmHg			
Prestimulation	74±6	106±15*	0.0011
During stimulation	78±6	110±17*	0.0023
Difference†	4.7±3.6	4.1±5.4	0.71
CSNA, μV			
Prestimulation	0.91±0.71 (100%)	0.98±0.78 (99±19%)	0.22
Poststimulation	0.93±0.72 (101±4%)	1.02±0.81 (104±21%)	0.18

Data are means ± SD values; $n = 7$ except for CSNA data where $n = 5$. †The difference was calculated by subtracting the prestimulation value from the value obtained during the sympathetic stimulation period in each animal. *$P < 0.01$ based on a paired *t*-test. Exact *P* values are also shown.

DISCUSSION

Intravenous administration of ANG II at 10 $\mu g \cdot kg^{-1} \cdot h^{-1}$ increased AP but did not affect mean HR or mean CSNA during prestimulation baseline conditions (Tables 1 and 3), suggesting that ANG II at this dose did not affect the residual sympathetic tone to the heart significantly. ANG II significantly attenuated the dynamic gain of the transfer function from vagal stimulation to HR, whereas it only slightly attenuated that of the transfer function from sympathetic stimulation to HR (Tables 2 and 4).

Effects of ANG II on the transfer function from vagal stimulation to HR. ANG II attenuated the dynamic gain of the transfer function from vagal stimulation to HR without affecting the corner frequency or pure delay (Fig. 2 and Table 2). Several interventions can affect the dynamic gain of the vagal transfer function and significantly change the corner frequency. For example, inhibition of cholinesterase, which interferes with the rapid hydrolysis of ACh, augments the dynamic gain and decreases the corner frequency (29). Moreover, blockade of muscarinic K^+ channels, which interferes with fast, membrane-delimited signal transduction, has been shown to attenuate the dynamic gain and decrease the corner frequency (26).

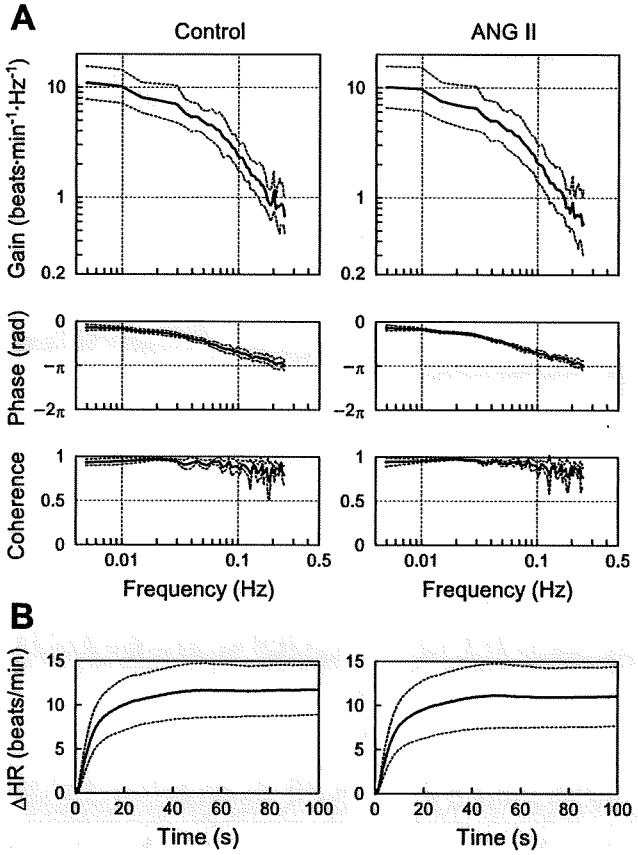

Fig. 4. *A*: averaged transfer functions from cardiac sympathetic nerve stimulation to the HR response obtained before and during intravenous administration of ANG II. Gain plots (*top*), phase plots (*middle*), and coherence plots (*bottom*) are shown. *B*: step responses of the HR to a unit change in the sympathetic stimulation calculated using the transfer functions. ΔHR, changes in heart rate. Solid lines indicate mean, and dashed lines indicate mean ± SD.

On the other hand, several other interventions have been shown to alter the dynamic gain of the vagal transfer function without changing the corner frequency. Concomitant cardiac sympathetic nerve stimulation or increased intracellular cyclic AMP levels augments the dynamic gain without affecting the corner frequency (14, 27), whereas β-adrenergic blockade or high plasma NE attenuates the dynamic gain without affecting the corner frequency (24, 25). Because α-adrenergic blockade nullifies its effects, high plasma NE probably functions via

Table 4. *Effects of intravenous ANG II administration on the parameters of the transfer function and the step response relating to the dynamic sympathetic control of HR*

	Control	ANG II	*P* Value
Dynamic gain, beats·min^{-1}·Hz^{-1}	10.8±2.6	10.2±3.1*	0.049
Natural frequency, Hz	0.069±0.009	0.065±0.006	0.090
Damping ratio	1.53±0.25	1.48±0.21	0.26
Pure delay, s	0.51±0.31	0.42±0.18	0.20
Goodness of fit, %	97.0±1.6	96.9±1.7	0.67
Steady-state response, beats/min	11.8±2.8	11.1±3.4	0.052
80% Rise time, s	17.2±4.7	16.8±4.5	0.62

Data are means ± SD; $n = 7$. *$P < 0.05$ based on a paired *t*-test. Exact *P* values are also shown.

Table 5. *Time effects on the parameters of the transfer function and the step response relating to the dynamic sympathetic control of HR*

	Control 1	Control 2	*P* Value
Dynamic gain, beats·min^{-1}·Hz^{-1}	9.1±1.7	8.6±2.4	0.37
Natural frequency, Hz	0.062±0.014	0.065±0.017	0.10
Damping ratio	1.36±0.22	1.34±0.28	0.75
Pure delay, s	0.65±0.32	0.56±0.25	0.12
Goodness of fit, %	95.8±4.0	97.3±2.2	0.32
Steady-state response, beats/min	9.8±2.0	9.5±2.8	0.55
80% Rise time, s	15.7±3.4	14.4±3.8	0.37

Data are means ± SD; $n = 7$. Exact *P* values are shown.

α-adrenergic receptors on preganglionic and/or postganglionic vagal nerve terminals to limit ACh release during vagal stimulation (24). Our observation that ANG II attenuated the dynamic gain without affecting the corner frequency or pure delay is similar to the results observed with high plasma NE, suggesting that ANG II limits ACh release during vagal stimulation. Although estimated values of the corner frequency ranged from 0.1 to 0.4 among studies, the difference may be attributable to the difference in the input signal properties (see Appendix B for details).

Although Andrews et al. (2) reported that ANG II (500 ng/kg, iv bolus) did not inhibit vagally induced bradycardia in anesthetized ferrets, Potter (31) demonstrated that ANG II (5–10 μg, iv bolus; body weight not shown) attenuated vagally induced bradycardia in anesthetized dogs. The latter study also showed that the addition of ANG II (2–5 μg/25 ml) to an organ bath attenuated vagally induced bradycardia in isolated guinea-pig atria. In that study, ANG II did not attenuate ACh-induced bradycardia, suggesting that the inhibition of bradycardia by ANG II was due to an inhibition of ACh release from vagal nerve terminals (31). In a previous study, we confirmed that intravenous ANG II (10 μg·kg^{-1}·h^{-1}) attenuated myocardial interstitial ACh release in response to vagal nerve stimulation in anesthetized cats (17). The site of this inhibitory action was thought to be parasympathetic ganglia rather than postganglionic vagal nerve terminals, because losartan, an antagonist of the ANG II receptor subtype 1 (AT_1 receptor), abolished the inhibitory action of ANG II when it was administered intravenously but not when it was administered locally through a dialysis fiber. ANG II may also function at the coronary endothelium and produce a diverse range of paracrine effects (6). Although the exact mechanisms remain to be elucidated, intravenous ANG II inhibits ACh release and thereby attenuates the dynamic gain of the vagal transfer function without affecting the corner frequency or pure delay.

Although the observed attenuation of the dynamic HR response to vagal stimulation by ANG II is relatively small, it may have pathophysiological significance as follows. In a previous study, our laboratory has shown that chronic intermittent vagal stimulation significantly improved the survival of chronic heart failure rats after myocardial infarction (21). In that study, the vagal stimulation intensity was such that it reduced HR only by 20 to 30 beats/min (5–10%) in rats. Therefore, change in the vagal effects on the heart, even if relatively small, could affect the evolution of heart failure. Increased plasma or tissue levels of ANG II in heart failure